Electronic Supporting Information (ESI)

A Tight Binding Pocket in Photoluminescent N^C^N Cyclometalated Pt(II), Pd(II), and Ni(II) Complexes

Maryam Niazi[a], Iván Maisuls[b], Cristian A. Strassert*[,b], Pablo González-Herrero[c], and Axel Klein*[,a]

[a] University of Cologne, Faculty for Mathematics and Natural Sciences, Department of Chemistry and Biochemistry, Institute for Inorganic Chemistry and Materials Chemistry, Greinstrasse 6, D-50939 Köln, Germany.
[b] Universität Münster, Institut für Anorganische und Analytische Chemie, Corrensstr. 28/30, D-48149 Münster, Germany; CeNTech, CiMIC, SoN, Heisenbergstr. 11, D-48149 Münster, Germany.
[c] Departamento de Química Inorgánica, Facultad de Química, Universidad de Murcia, Campus de Espinardo 19, 30100 Murcia, Spain.

Contents

Fig. S24 Photoluminescence emission and excitation spectra of [Pt(L^{Bn})Cl] in solid state at 298 K and at 77 K (λ_{ex} = 400 nm).
Fig. S25 Photoluminescence spectra of [Pt(L^{Bn})Cl] at different concentrations within PMMA films at 298 K (λ_{ex} = 400 nm).
Fig. S26 Photoluminescence emission spectrum of HL^{Bn} in a frozen glassy matrix (2-MeTHF, $c = 10^{-5}$ M, λ_{ex} = 350 nm).
Fig. S27 DFT-calculated energies of the lowest singly occupied (LSOMO, black) and highest singly occupied (LSOMO, red) molecular orbitals for [M(L^{Bn})Cl] (M = Pt, Pd, and Ni).
Fig. S28 Left: Raw (experimental) time-resolved photoluminescence decay of [Pt(L^{Bn})Cl] in fluid CH_2Cl_2 at 298 K (air-equilibrated, λ_{ex} = 376 nm, λ_{em} = 580 nm) including the residuals. Right: Fitting parameters including pre-exponential factors and confidence limits.
Fig. S29 Left: Raw (experimental) time-resolved photoluminescence decay of [Pt(L^{Bn})Cl] in fluid CH_2Cl_2 at 298 K (Ar-purged, λ_{ex} = 376 nm, λ_{em} = 580 nm) including the residuals. Right: Fitting parameters including pre-exponential factors and confidence limits.
Fig. S30 Raw (experimental) time-resolved photoluminescence decay with the fitting parameters including pre-exponential factors and confidence limits of [Pt(L^{Bn})Cl] as a crystal at 298 K.
Fig. S31 Left: Raw (experimental) time-resolved photoluminescence decay of [Pt(L^{Bn})Cl] in a frozen glassy 2-MeTHF matrix (V:V = 1:1) at 77 K, including the residuals (λ_{exc} = 376.7 nm, λ_{em} = 495 nm). Right: Fitting parameters including pre-exponential factors and confidence limits.
Fig. S32 Left: Raw (experimental) time-resolved photoluminescence decay of [Pd(L^{Bn})Cl] in a frozen glassy 2-MeTHF matrix (V:V = 1:1) at 77 K, including the residuals (λ_{exc} = 376.7 nm, λ_{em} = 700 nm). Right: Fitting parameters including pre-exponential factors and confidence limits.
Fig. S33 Left: Raw (experimental) time-resolved photoluminescence decay of [Ni(L^{Bn})Cl] in a frozen glassy 2-MeTHF matrix (V:V = 1:1) at 77 K, including the residuals (λ_{exc} = 376.7 nm, λ_{em} = 530 nm). Right: Fitting parameters including pre-exponential factors and confidence limits.
Fig. S34 Left: Time-resolved photoluminescence decay (blue) of HL^{Bn} and the instrument response function (IRF, red) in a frozen glassy matrix of 2-MeTHF at 77 K, including the residuals (λ_{ex} = 376 nm, λ_{obs} = 475 nm). **Right**: Fitting parameters including pre-exponential factors and confidence limits.
Fig. S35 Left: Time-resolved photoluminescence decay (blue) of ClL^{Bn} and the instrument response function (IRF, red) in a frozen glassy matrix of 2-MeTHF at 77 K, including the residuals (λ_{ex} = 376 nm, λ_{obs} = 475 nm). Right: Fitting parameters including pre-exponential factors and confidence limits.

Supporting Tables

Table S1 Crystal data and structure refinement for the [M(L^{Bn})Cl] (M = Pt or Pd) and [Ni(L^{Bn})Cl]·½CH_2Cl_2.
Table S2 Experimental and DFT-calculated geometries of [M(L^{Bn})Cl] (M = Pt, Pd, Ni).
Table S3 Redox potentials of the complexes [M(L^{Bn})Cl] (M = Pt, Pd, and Ni).
Table S4 Selected UV-Vis absorption maxima of the complexes [M(L^{Bn})Cl] (M = Pt, Pd, and Ni).
Table S5 DFT-calculated energies and compositions of frontier MOs in the S_0 ground state for [M(L^{Bn})Cl] (M = Pt, Pd, and Ni).
Table S6 DFT-calculated energies and compositions of frontier MOs in the T_1 excited state for [M(L^{Bn})Cl] (M = Pt, Pd, and Ni).
Table S7 Selected TD-DFT-calculated vertical $S_0 \rightarrow S_n$ transitions for [M(L^{Bn})Cl] (M = Pt, Pd, and Ni).
Table S8 Photophysical properties of [Pt(L^{Bn})Cl] complex at 298 K.
Table S9 Calculated coordinates of the optimised singlet ground state structures of the complexes [M(L^{Bn})Cl] (M = Pt, Pd, and Ni).
Table S10 Calculated coordinates of the optimised triplet excited state structures of the complexes [M(L^{Bn})Cl] (M = Pt, Pd, and Ni).

Syntheses of the Ligand Precursors

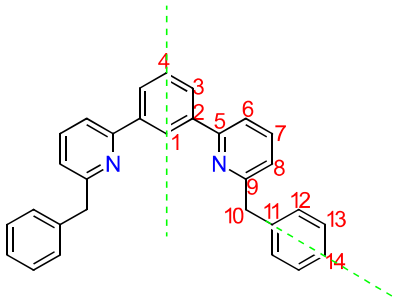

Scheme S1 Numbering schemes used in the NMR assignments.

1.1 Synthesis of the N^C^N ligand precursor HL^{Bn}

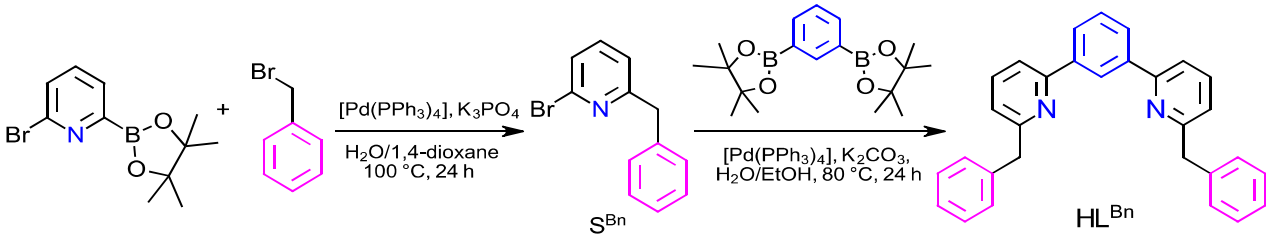

Scheme S2 Synthetic pathway for HL^{Bn}.

Synthesis of 2,2′-(1,3-phenylene)bis,(4,4,5,5-tetramethyl-1,3,2-dioxaborolane) (or 1,3-phenyldiboronic acid, pinacol ester). To a solution of 1,3-dibromobenzene (4.2 mmol, 1.0 g), B_2Pin_2 (12.7 mmol, 3.2 g), and KOAc (21.2 mmol, 2.1 g), in 15 mL 1,4-dioxane was added $[Pd(PPh_3)_2Cl_2]$ (6 mol%, 0.179 g) under inert condition. After three freeze-thaw cycles to remove trace amount of oxygen, the reaction mixture stirred at 102 °C for 12 h. The mixture was cooled down and 10 mL EtOAc was added to quench the reaction. The organic phase was washed with brine solution (3 × 10 mL) and dried over anhydrous Na_2SO_4. After evaporation of the solvent, crude product was purified by column chromatography using CH_2Cl_2 as an eluent to give white crystals. Yield: 1.420 g (3.9 mmol, 92%). ^{1}H NMR (300 MHz, $CDCl_3$, 298 K): δ /ppm = 8.27 (s, 1H), 7.89 (dd, J = 7.4, 1.4 Hz, 2H), 7.37 (td, J = 7.4, 0.8 Hz, 1H), 1.33 (s, 24H).

Synthesis of S^{Bn}. 2-Bromopyridine-6-boronic acid pinacol ester (0.500 g, 1.76 mmol), benzyl bromide (0.190 mL, 1.6 mmol), $[Pd(PPh_3)_4]$ (0.111 g, 6 mol%), and K_3PO_4 (0.679 g, 3.2 mmol) were mixed and dissolved in 25 mL H_2O/1,4-dioxane (1:1, degassed). The solution was stirred for 24 h at 100 °C under an argon atmosphere. After allowing the reaction mixture to cool to room temperature, the mixture was filtered and diluted with 15 mL EtOAc. The resulting solution was washed with brine (2 × 20 mL), separated and dried over anhydrous Na_2SO_4. The crude product was purified by column chromatography with *n*-Hex:EtOAc (9:1 v/v). Yield: 0.240 g (0.967 mmol, 60%). ^{1}H NMR (500 MHz, acetone-d_6, 298 K): δ /ppm = 7.57 (t, J = 7.7 Hz, 1H), 7.39 (dd, J = 7.9, 0.7 Hz, 1H), 7.30 (d, J = 4.5 Hz, 4H), 7.24 – 7.19 (m, 2H), 4.09 (s, 2H). ^{13}C NMR (126 MHz, acetone-d_6, 298 K): δ /ppm = 163.39, 141.91, 140.22, 139.86, 129.78, 129.28, 127.19, 126.32, 122.92, 44.38.

Synthesis of HL^{Bn}. 1,3-phenyldiboronic acid bis(pinacol)ester (0.407 g, 1.23 mmol), S^{Bn} (0.437 g, 1.76 mmol), $[Pd(PPh_3)_4]$ (0.122 g, 6 mol%), and K_2CO_3 (0.486 g, 3.52 mmol) were mixed and dissolved in 20 mL H_2O/EtOH (1:1, degassed). The solution was stirred for 24 h at 80 °C under an argon atmosphere. After allowing the reaction mixture to cool to room temperature, the mixture was filtered and diluted with 15 mL CH_2Cl_2. The resulting solution was washed with brine (3 × 20 mL), separated and dried over anhydrous Na_2SO_4. The crude product was purified by column chromatography with *n*-Hex:EtOAc (8:2 v/v). Yield: 0.298 g (0.72 mmol, 82%). ^{1}H NMR (600 MHz, DMSO-d_6, 298 K): δ /ppm = 8.78 (t, J = 1.8 Hz, 1H, H1), 8.13 (dd, J = 7.7, 1.8 Hz, 2H, H3), 7.86 (dd, J = 7.8, 1.0 Hz, 2H, H6), 7.81 (t, J = 7.7 Hz, 2H, H7), 7.60 (t, J = 7.7 Hz, 1H, H4), 7.40 – 7.34 (m, 4H, H12), 7.34 – 7.26 (m, 4H, H13), 7.25 (dd, J = 7.5, 1.0 Hz, 2H, H8), 7.23 – 7.17 (m, 2H, H14), 4.19 (s, 4H, H10). ^{13}C NMR (151 MHz, DMSO-d_6, 298 K): δ /ppm = 160.44 (C9), 155.31 (C2), 139.79 (C11), 139.17 (C5), 137.83 (C7), 129.12 (C4), 128.97 (C12), 128.39 (C13), 127.12 (C3), 126.15 (C14), 124.80 (C1), 121.83 (C8), 117.92 (C6), 43.97 (C10). HR-

ESI MS(+): calcd. for $[C_{30}H_{25}N_2]^+$ m/z = 413.20122; found m/z = 413.20091 $[M+H]^+$. Elemental analysis calcd. (%) for $C_{30}H_{24}N_2$, M = 412.52 g mol^{-1}: C, 87.35; H, 5.86; N, 6.79. Found C, 85.71; H, 5.72; N, 6.73.

1.2 Synthesis of the ligand precursor ClL^{Bn}

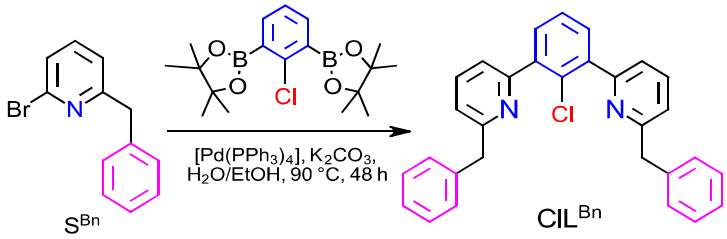

Scheme S3 Synthetic pathways for ClL^{Bn}.

Synthesis of 2,2′-(2-chloro-1,3-phenylene)bis,(4,4,5,5-tetramethyl-1,3,2-dioxaborolane) (or 2-chloro-1,3 phenyldiboronic acid, pinacol ester). To a solution of 1,3-dibromo-2-chlorobenzene (1.0 mmol, 0.270 g), B_2Pin_2 (3.0 mmol, 0.761 g), and KOAc (5 mmol, 0.491 g), in 6 mL 1,4-dioxane was added $[Pd(PPh_3)_2Cl_2]$ (6 mol%, 0.042 g) under inert condition. After three freeze-thaw cycles to remove trace amount of oxygen, the reaction mixture stirred at 102 °C for 12 h. The mixture was cooled down and 10 mL EtOAc was added to quench the reaction. The organic phase was washed with brine solution (3 × 20 mL) and dried over anhydrous Na_2SO_4. After evaporation of the solvent, crude product was purified by column chromatography using CH_2Cl_2 as an eluent to give white crystals. Yield: 0.272 g (0.75 mmol, 75%). ^{1}H NMR (300 MHz, acetone-d_6, 298 K): δ /ppm = 7.68 (d, J = 7.4 Hz, 2H), 7.29 (t, J = 7.4 Hz, 1H), 1.35 (s, 24H).

Synthesis of ClL^{Bn}. 2-chloro-1,3-Phenyldiboronic acid, pinacol ester (0.730 g, 2.00 mmol), S^{Bn} (0.710 g, 2.86 mmol), $[Pd(PPh_3)_4]$ (0.198 g, 6 mol%), and K_2CO_3 (0.791 g, 5.72 mmol) were mixed and dissolved in 40 mL H_2O/EtOH (1:1, degassed). The solution was stirred for 48 h at 90 °C under an argon atmosphere. After allowing the reaction mixture to cool to ambient temperature, the mixture was extracted with CH_2Cl_2. The extract was washed with brine (2 × 30 mL), separated and dried over anhydrous Na_2SO_4. The crude product was purified by column chromatography with n-Hex:EtOAc (8:2 v/v). Yield: 0.462 g (1.03 mmol, 72%). ^{1}H NMR (500 MHz, DMSO-d_6, 298 K): δ /ppm = 7.81 (t, J = 7.7 Hz, 2H, H3), 7.59–7.51 (m, 3H, H6 and H4), 7.47 (dd, J = 7.8, 1.0 Hz, 2H, H7), 7.35–7.26 (m, 10H, H12, H13 and H8), 7.23–7.16 (m, 2H, H14), 4.15 (s, 4H, H10). ^{13}C NMR (151 MHz, acetone-d_6, 298 K): δ /ppm = 161.69 (C9), 157.68 (C2), 150.07 (C1), 141.71 (C5), 140.93 (C4), 137.42 (C11), 132.30 (C7), 129.90 (C12), 129.26 (C13), 127.53 (C3), 127.03 (C14), 123.22 (C8), 122.61 (C6), 45.17 (C10). HR-ESI MS(+): calcd. for $[C_{30}H_{24}ClN_2]^+$ m/z = 447.16225; found m/z = 447.16240 $[M+H]^+$. Elemental analysis calcd. (%) for $C_{30}H_{23}ClN_2$, M = 446.97 g mol^{-1}: C, 80.61; H, 5.19; N, 6.27. Found C, 80.90; H, 5.63; N, 6.34.

Supporting Figures

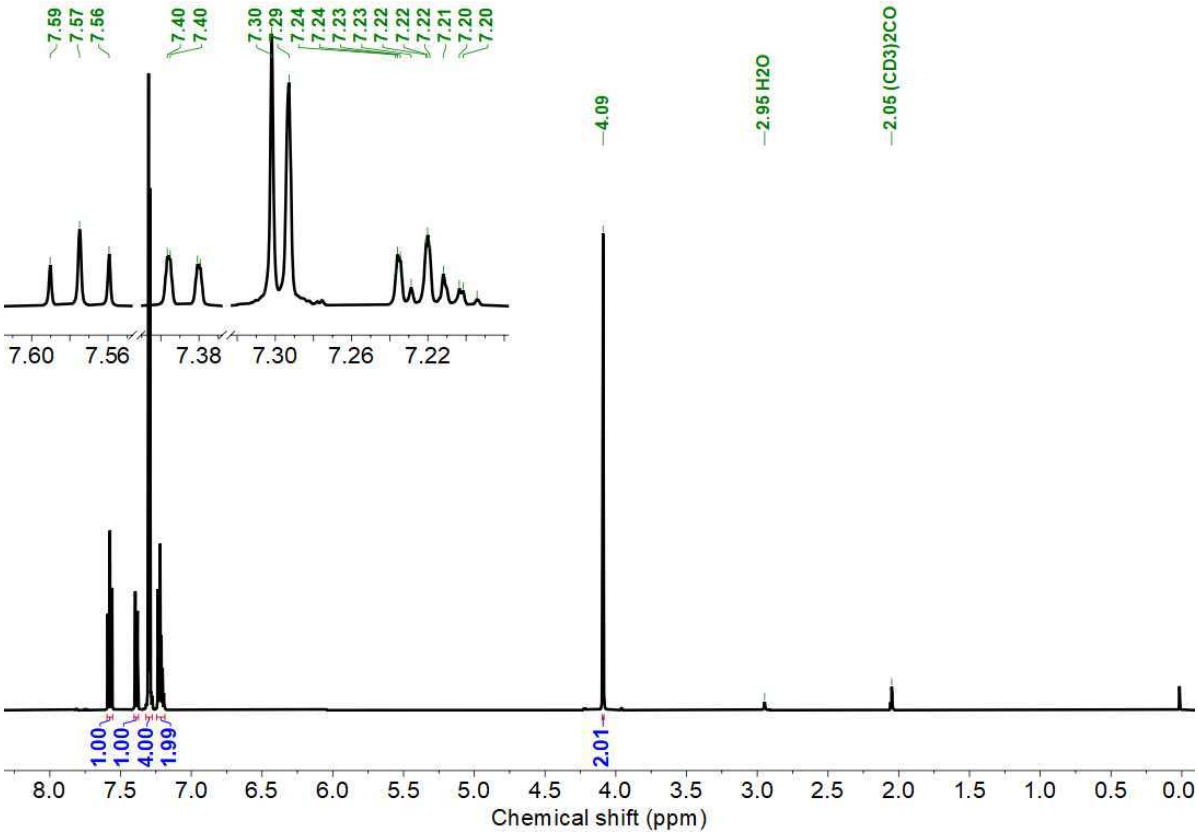

Fig. S1 500 MHz ^{1}H NMR spectrum of S^{Bn} in acetone-d_6 at RT.

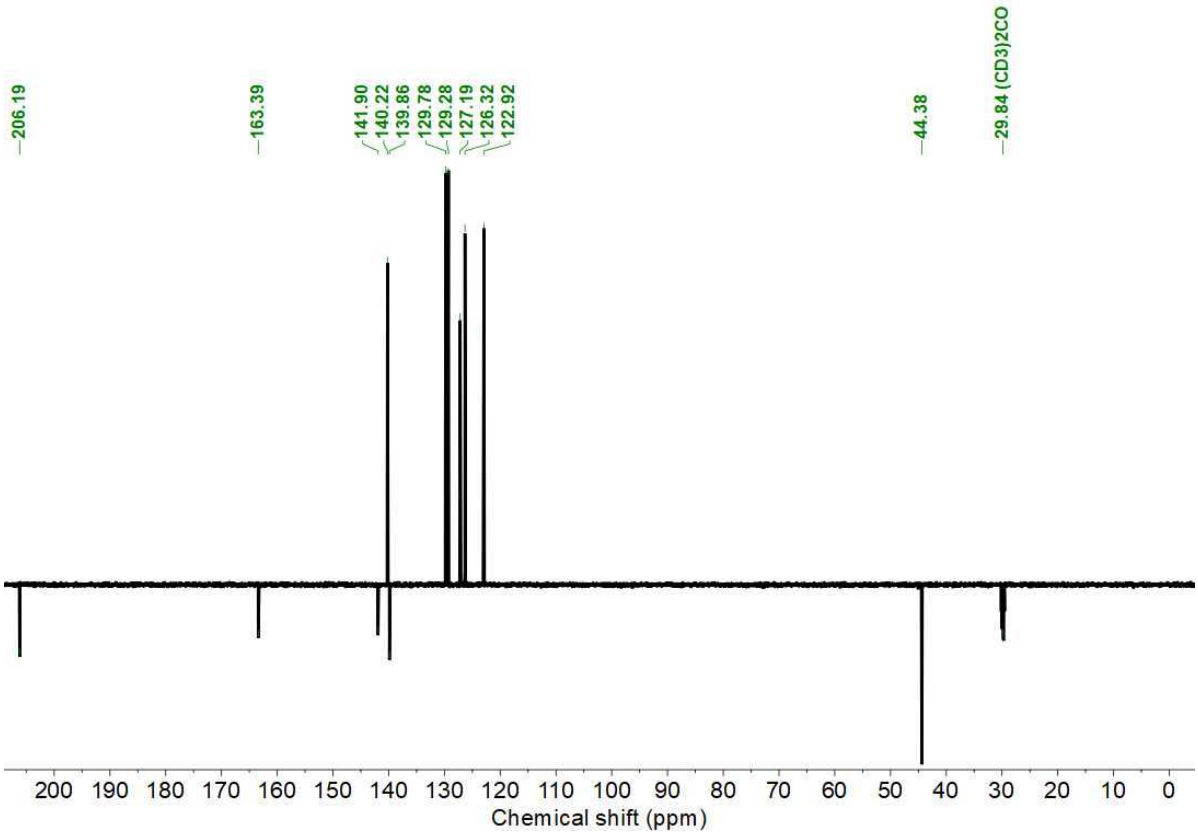

Fig. S2 126 MHz ^{13}C NMR spectrum of S^{Bn} in acetone-d_6 at RT.

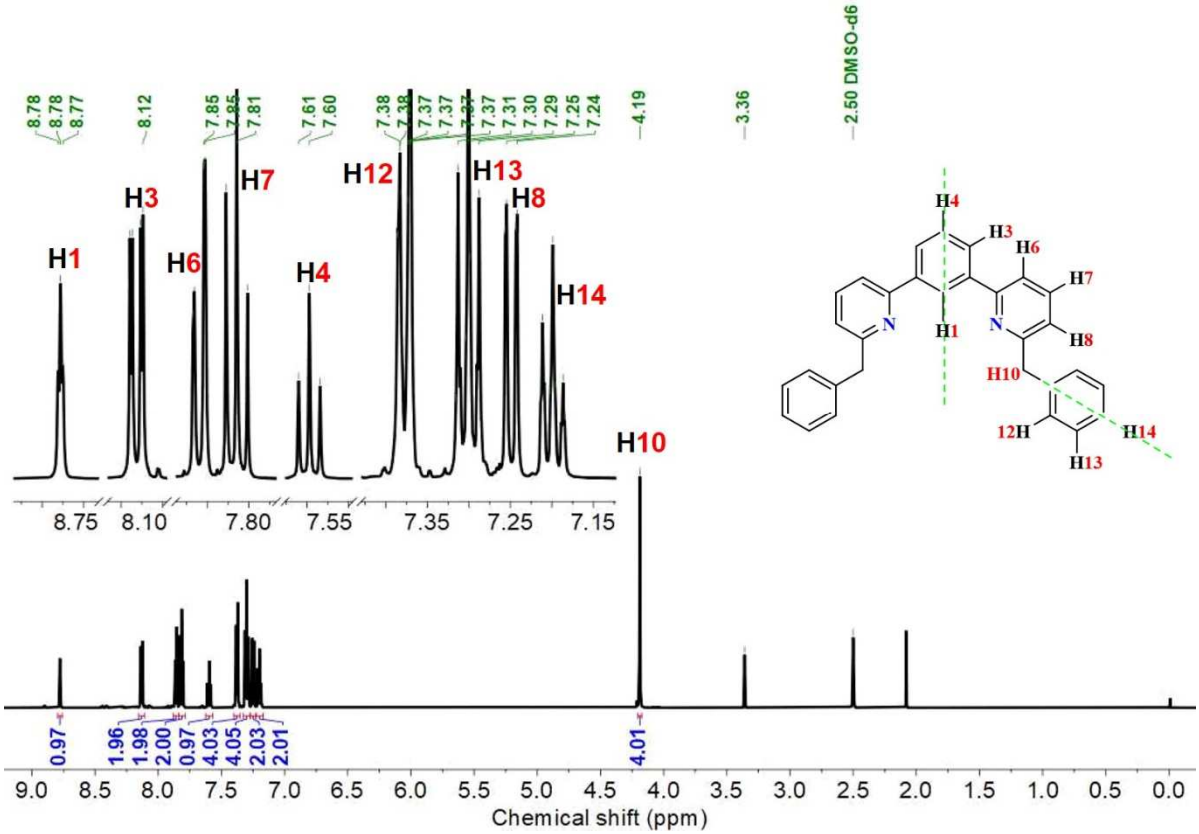

Fig. S3 600 MHz ^{1}H NMR spectrum of HL^{Bn} in DMSO-d_6 at RT.

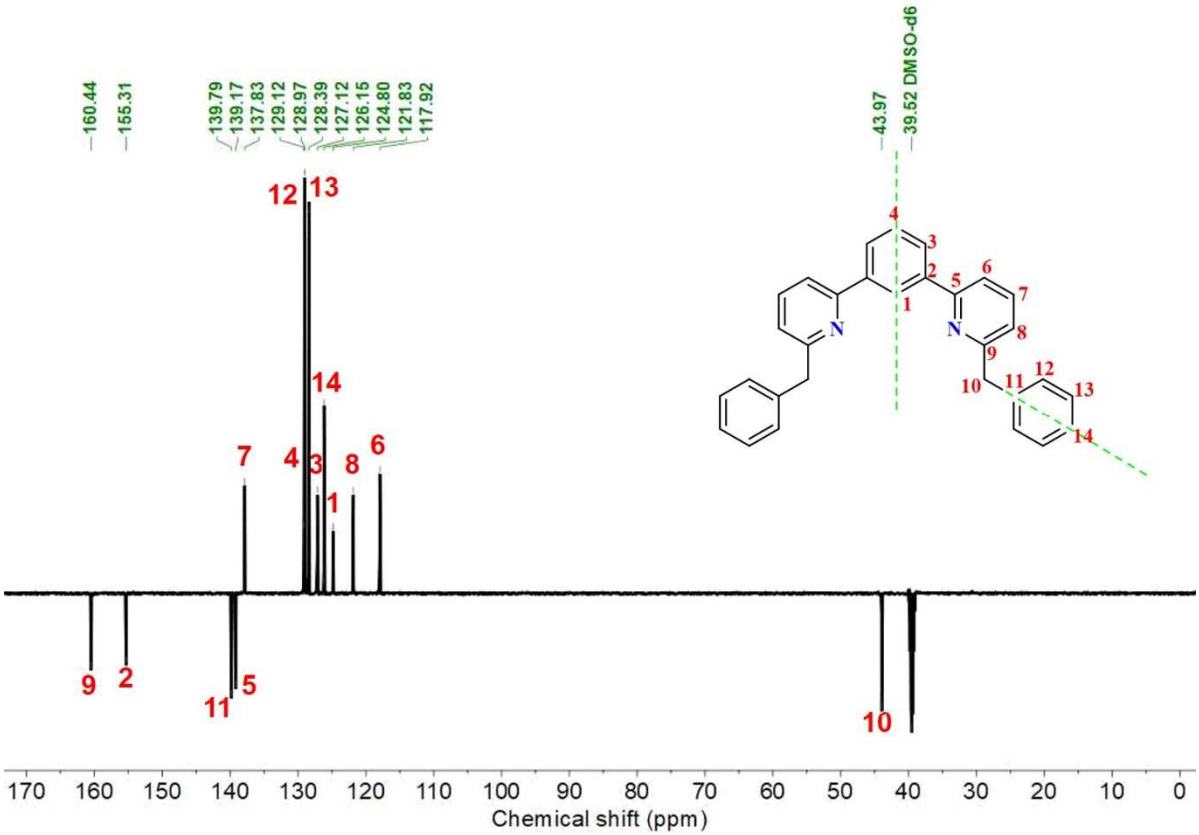

Fig. S4 151 MHz ^{13}C NMR spectrum of HL^{Bn} in DMSO-d_6 at RT.

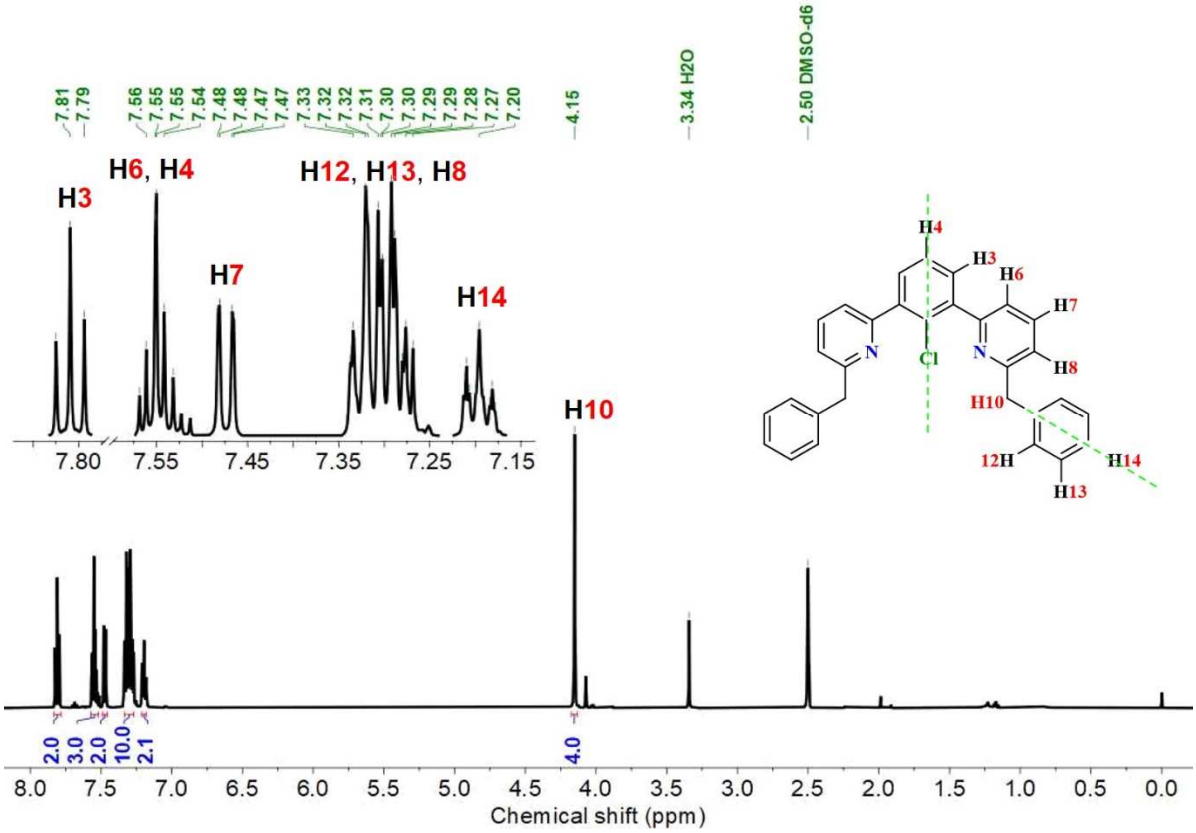

Fig. S5 500 MHz ^{1}H NMR spectrum of ClL^{Bn} in DMSO-d_6 at RT.

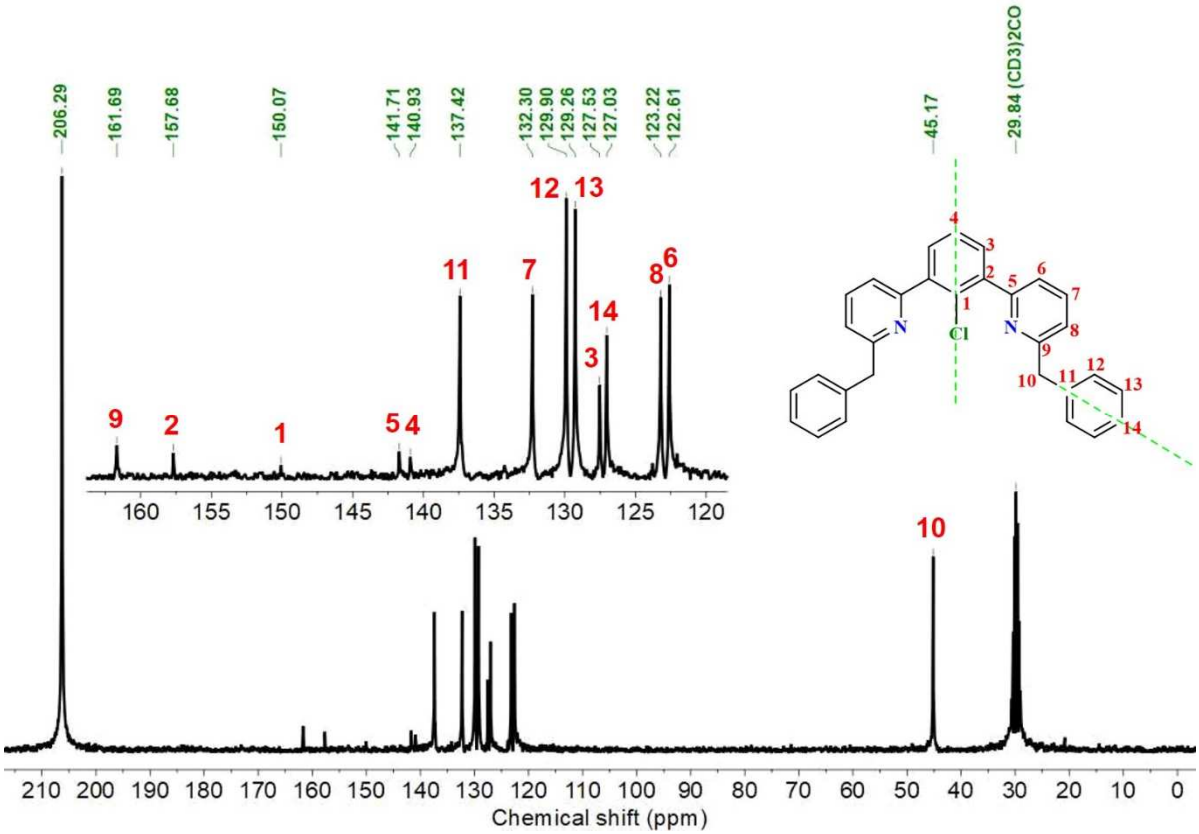

Fig. S6 151 MHz ^{13}C NMR spectrum of ClL^{Bn} in acetone-d_6 at RT.

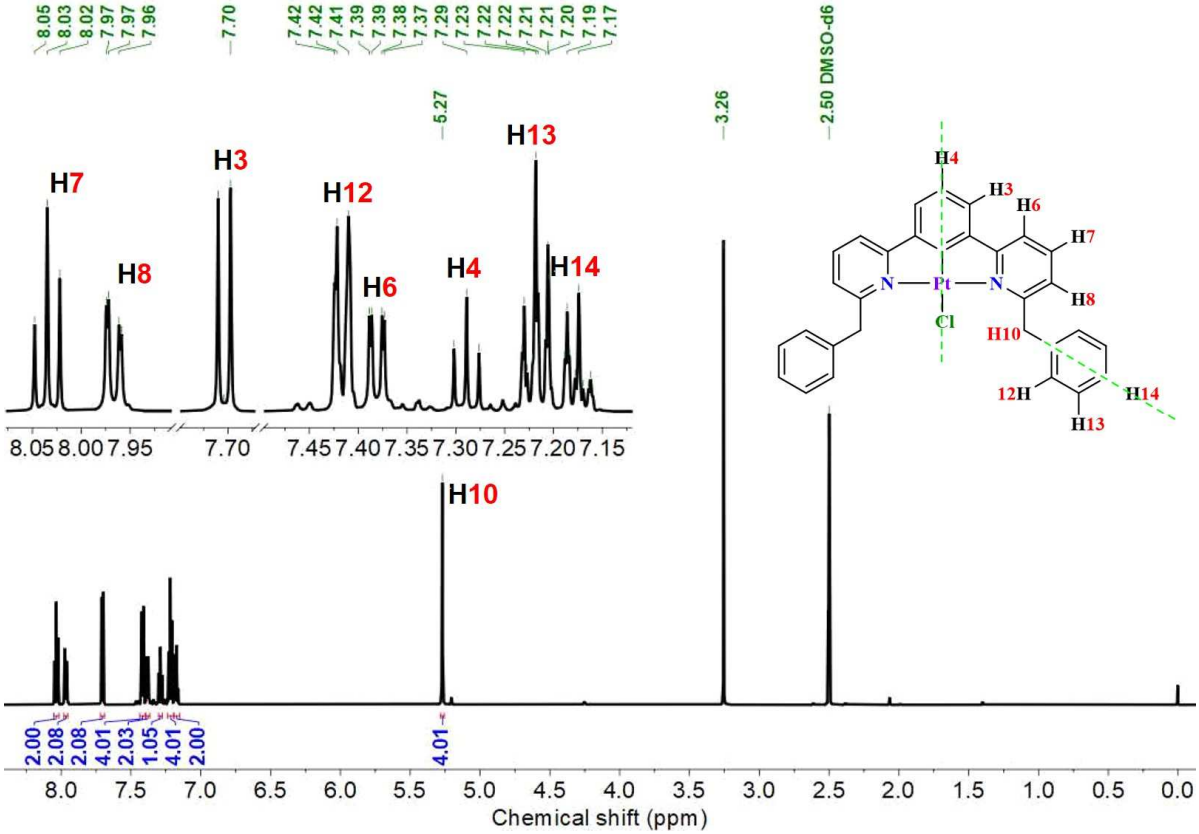

Fig. S7 600 MHz ^{1}H NMR spectrum of [Pt(L^{Bn})Cl] in DMSO-*d*$_6$ at RT.

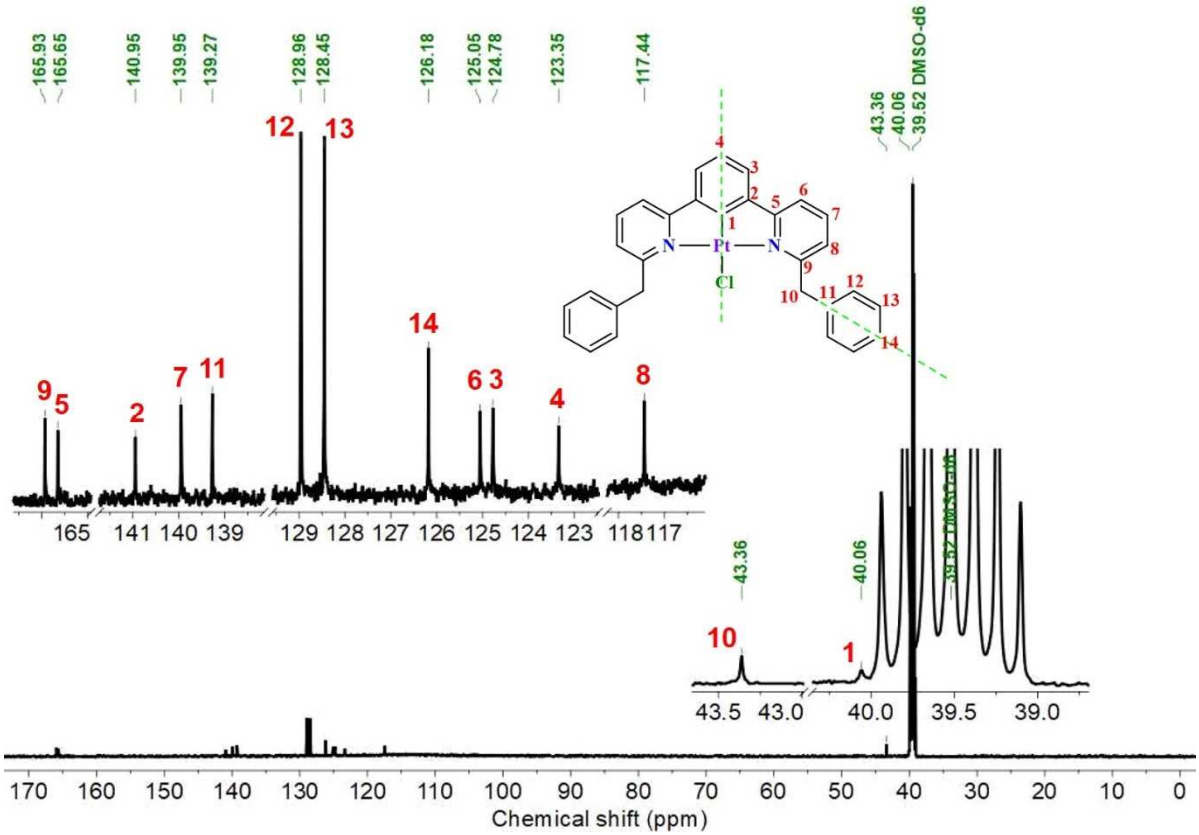

Fig. S8 151 MHz ^{13}C NMR spectrum of [Pt(L^{Bn})Cl] in DMSO-*d*$_6$ at 313 K.

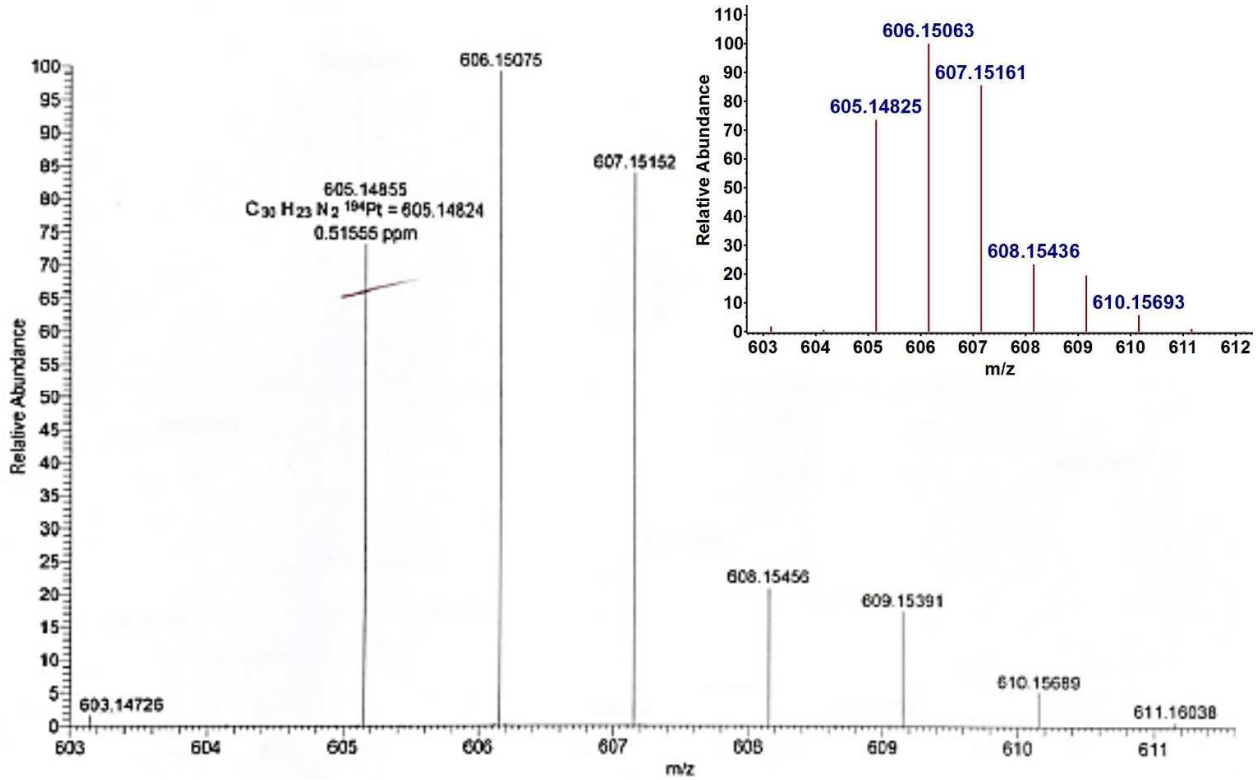

Fig. S9 High-resolution ESI-MS(+) spectrum of [Pt(L^{Bn})Cl] (black) and calculated pattern for [$C_{30}H_{23}N_2Pt$]$^+$ = [M-Cl]$^+$ (red).

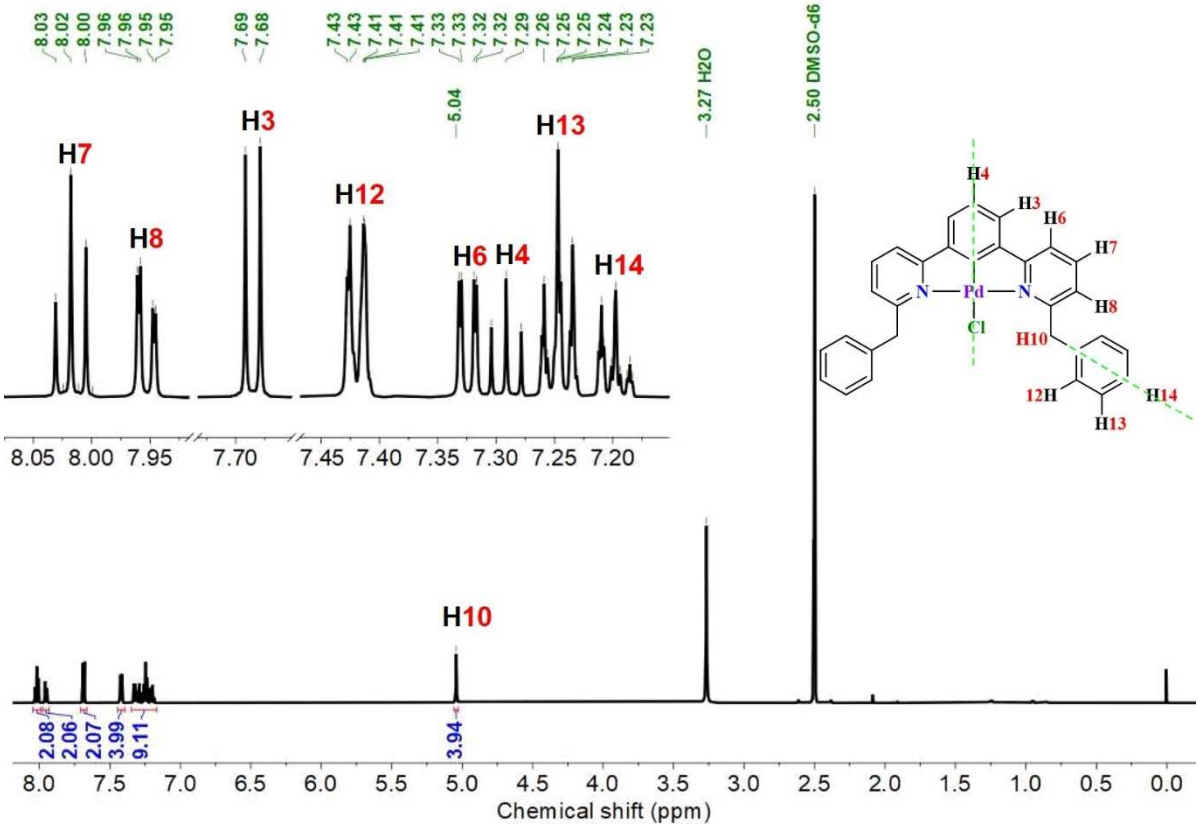

Fig. S10 600 MHz ^{1}H NMR spectrum of [Pd(L^{Bn})Cl] in DMSO-d_6 at RT.

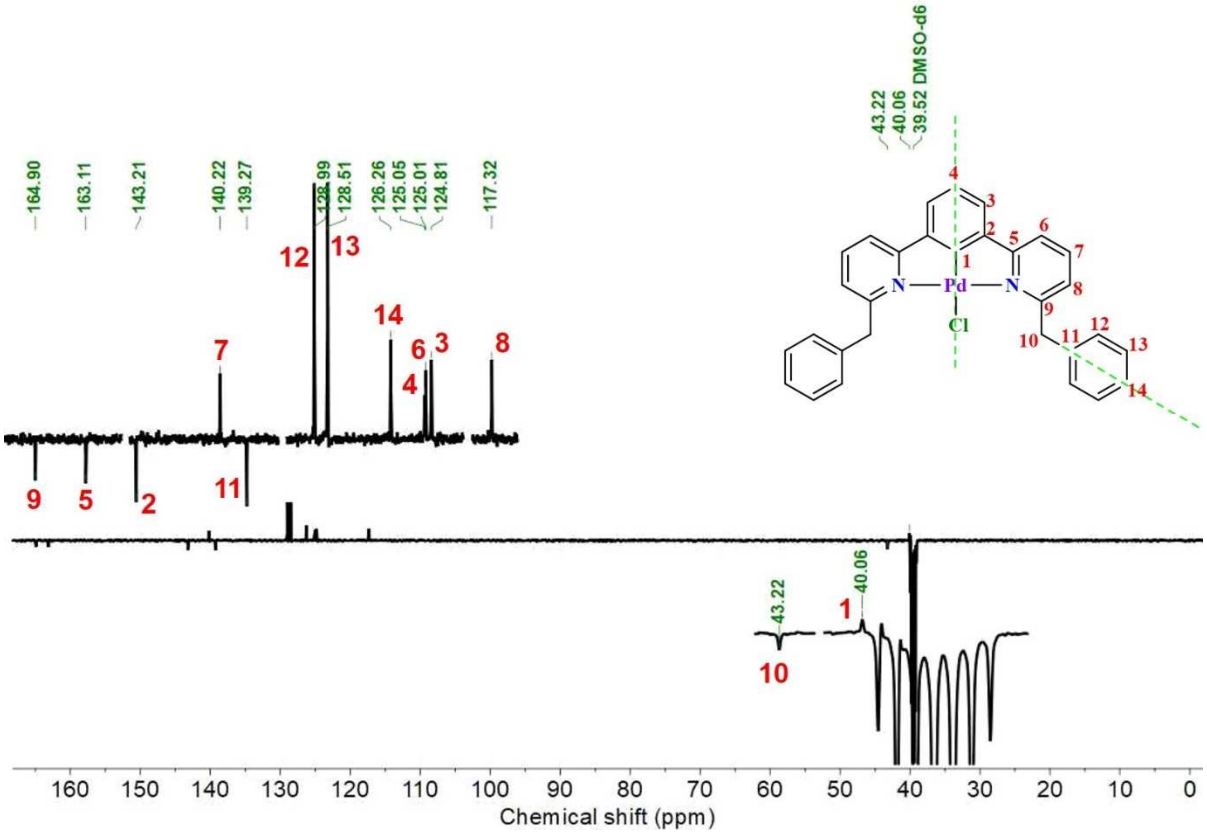

Fig. S11 151 MHz ^{13}C NMR spectrum of [Pd(L^{Bn})Cl] in DMSO-d_6 at 313 K.

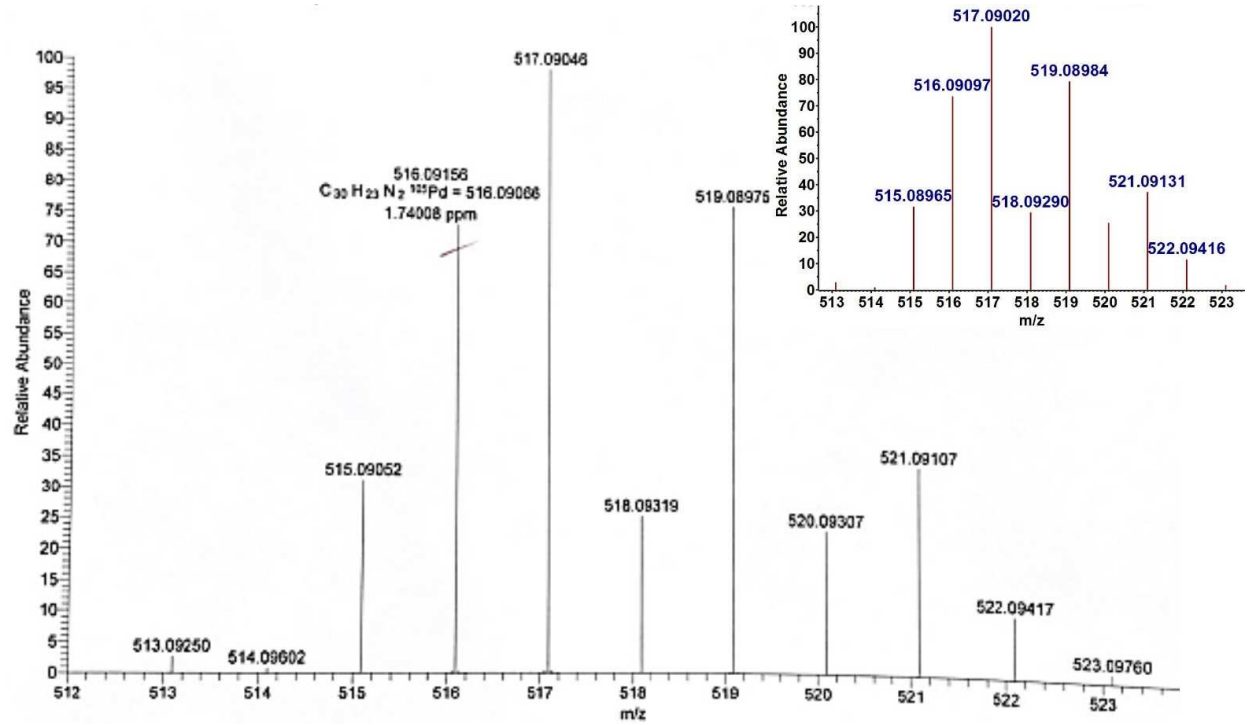

Fig. S12 High-resolution ESI-MS(+) spectrum of [Pd(L^{Bn})Cl] (black) and calculated pattern for [$C_{30}H_{23}N_2Pd$]$^+$ = [M-Cl]$^+$ (red).#

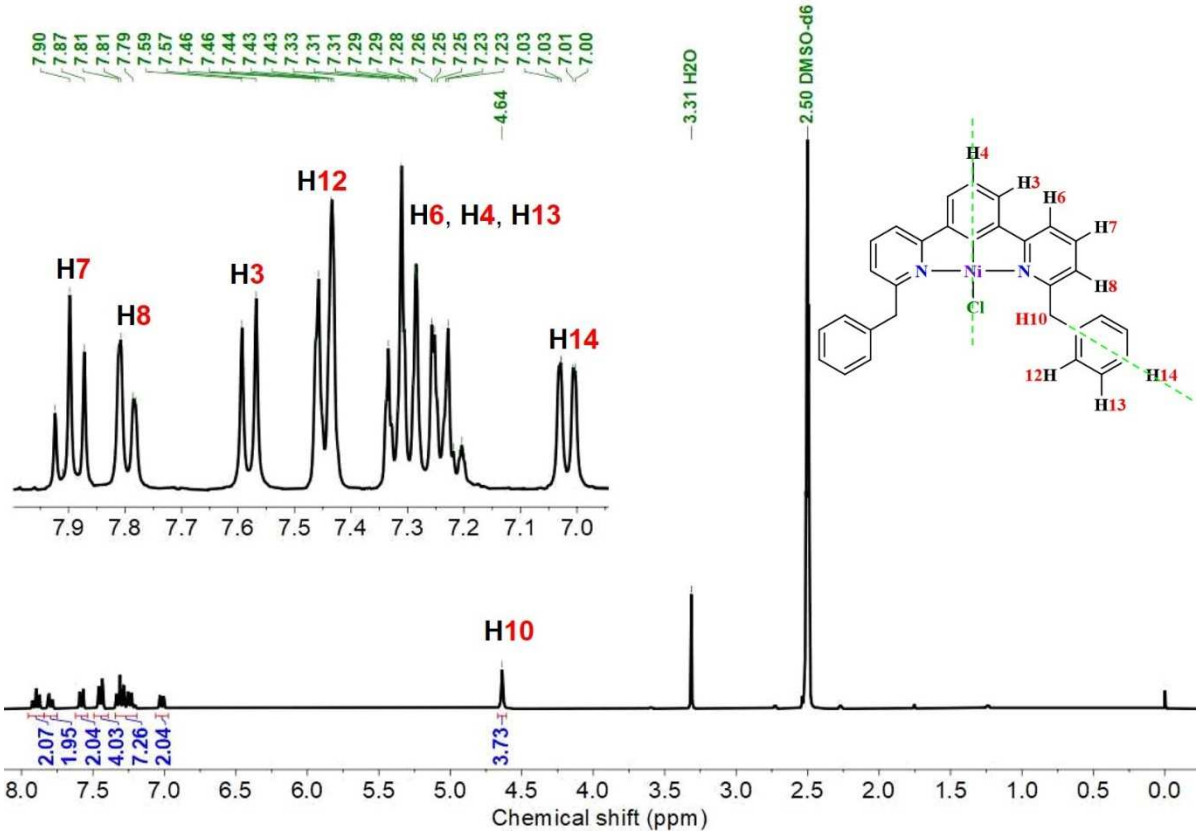

Fig. S13 300 MHz ^{1}H NMR spectrum of [Ni(L^{Bn})Cl] in DMSO-d_6 at RT.

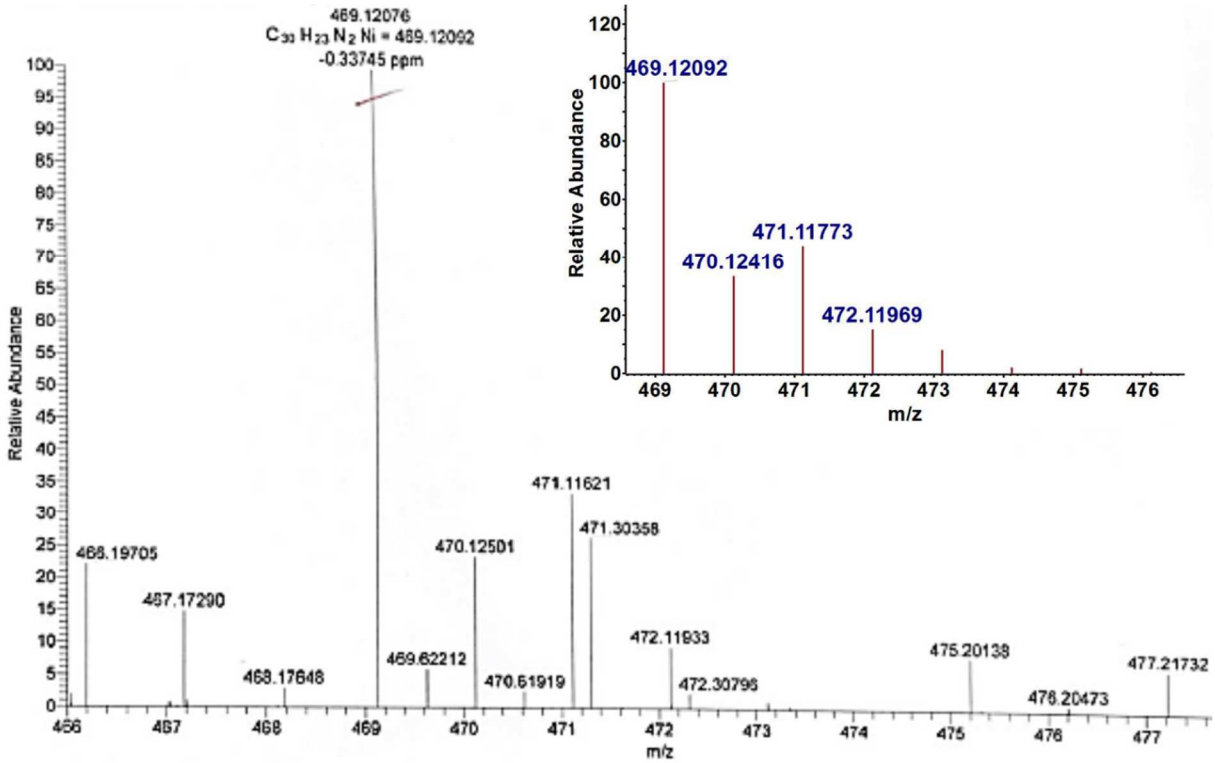

Fig. S14 High-resolution ESI-MS(+) spectrum of [Ni(L^{Bn})Cl] (black) and calculated pattern for $[C_{30}H_{23}N_2Ni]^+$ = $[M\text{-}Cl]^+$ (red).

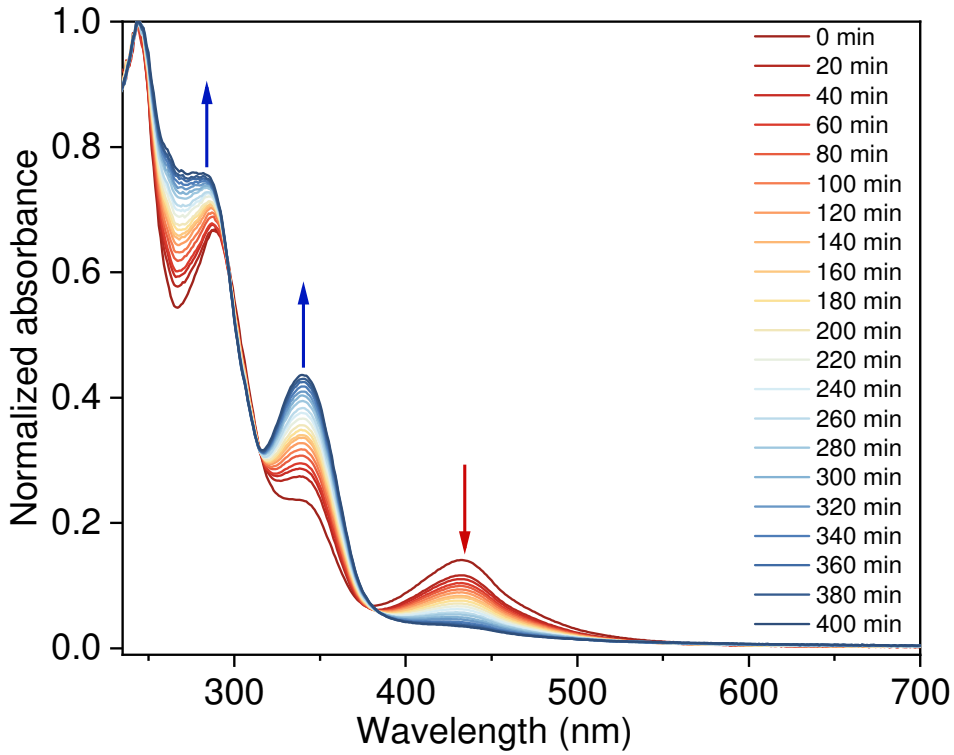

Fig. S15 UV-vis absorption spectra of the complex [Ni(L^{Bn})Cl] over time in THF solution at 298 K.

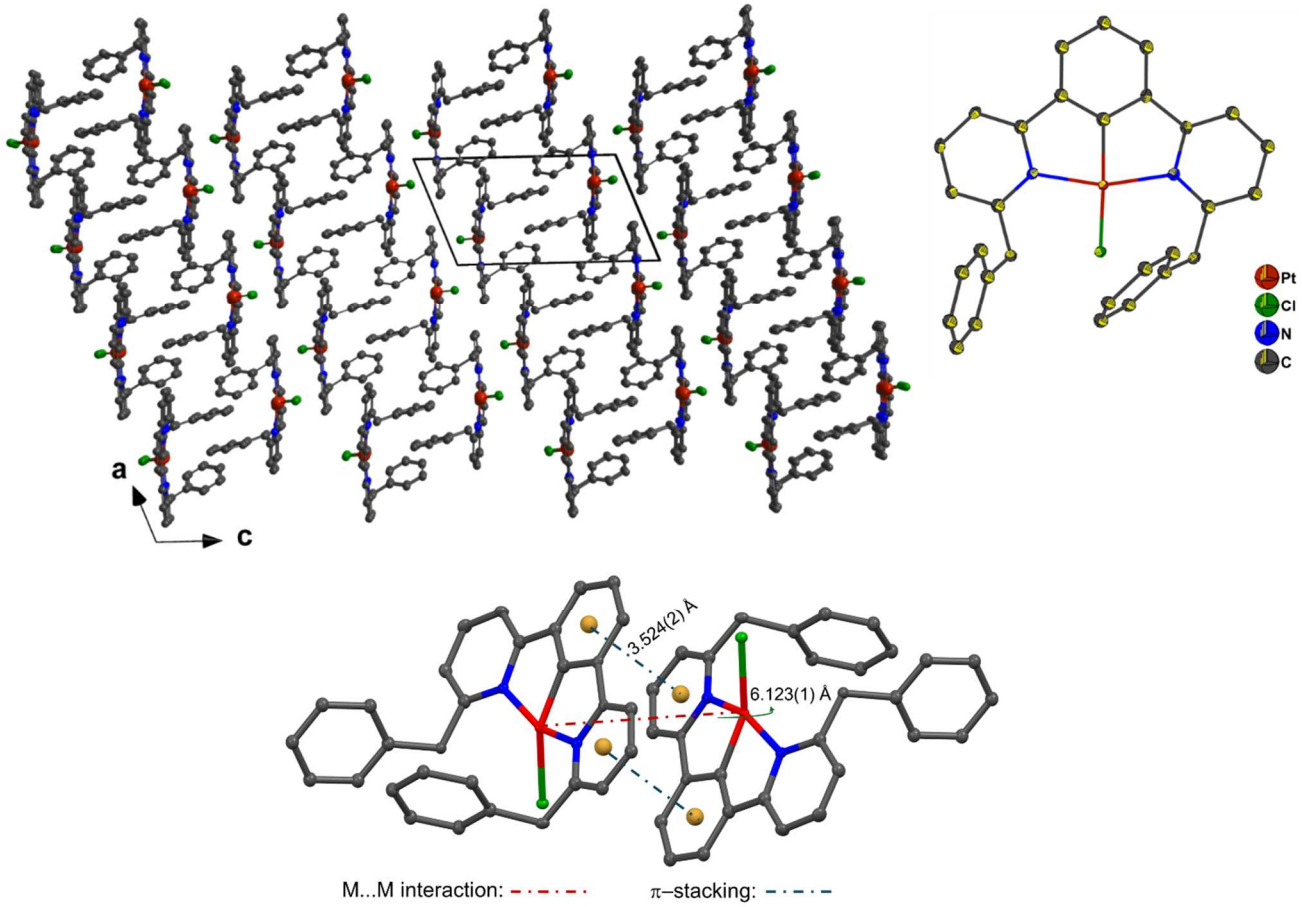

Fig. S16 Crystal structure of [Pt(L^{Bn})Cl] from single crystal XRD, viewed along the crystallographic *b* axis (top left) and molecular structure with atoms as 50% ellipsoids (top right), H atoms omitted for clarity, along with extended view of the packing of the complex showing the intermolecular interactions (bottom).

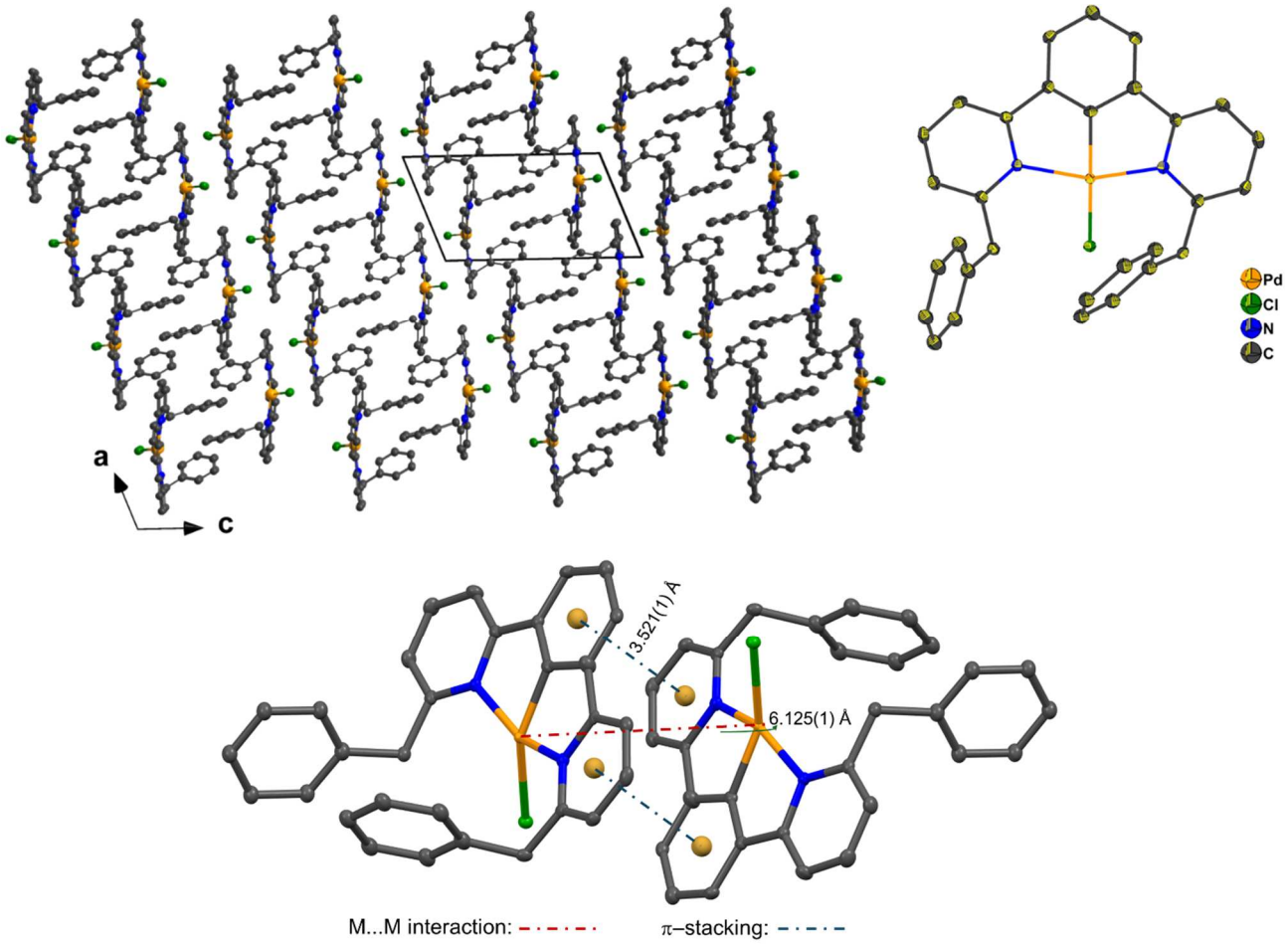

Fig. S17 Crystal structure of [Pd(L^{Bn})Cl] from single crystal XRD, viewed along the crystallographic *b* axis (top left) and molecular structure with atoms as 50% ellipsoids (top right), H atoms omitted for clarity, along with extended view of the packing of the complex showing the intermolecular interactions (bottom).

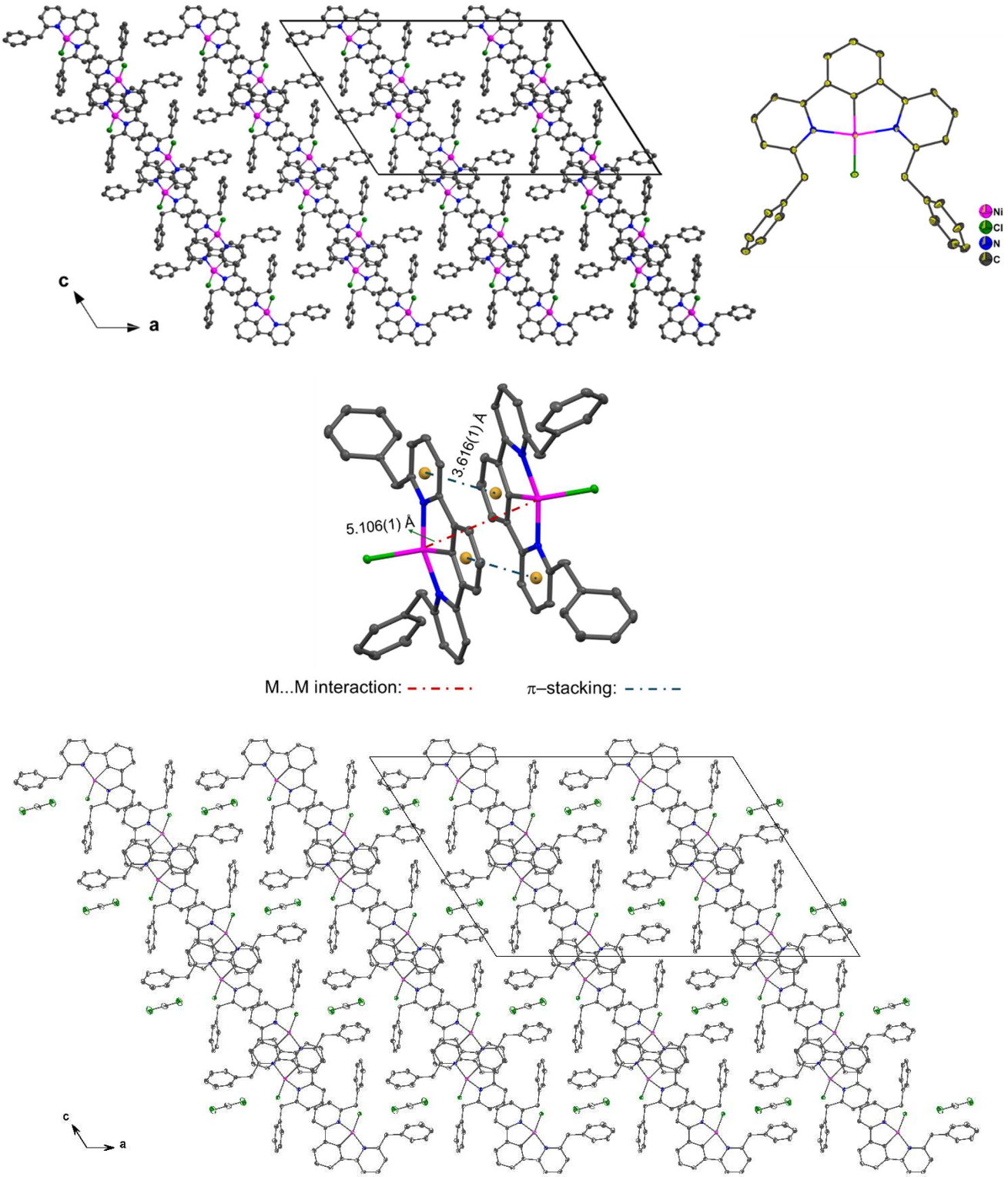

Fig. S18 Crystal structure of [Ni(L^{Bn})Cl] ½CH_2Cl_2 from single crystal XRD, viewed along the crystallographic *b* axis (top left) and molecular structure with atoms as 50% ellipsoids (top right). Extended view of the packing of the complex showing the intermolecular interactions (centre) and crystal structure of [Ni(L^{Bn})Cl] with co-crystallised CH_2Cl_2 molecules (bottom). H atoms omitted for clarity.

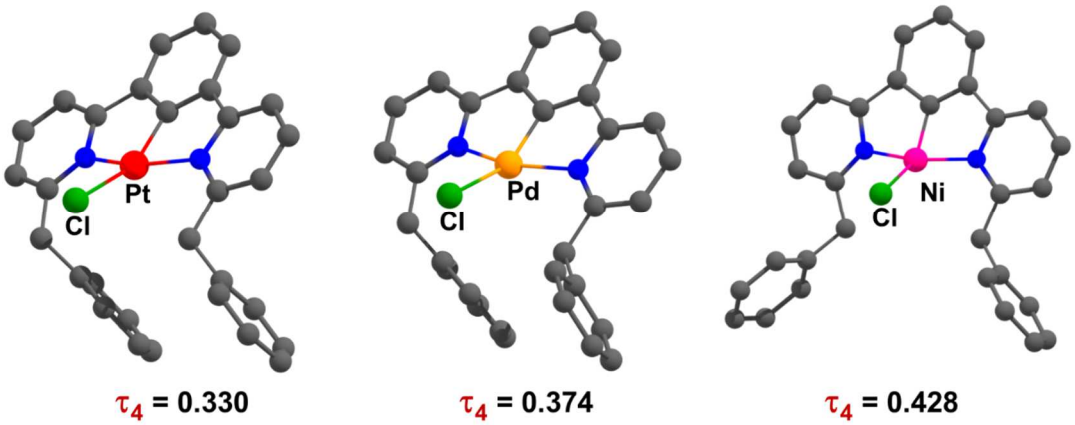

Fig. S19 DFT-calculated molecular structures of [M(L^{Bn})Cl] (M = Pt, Pd, and Ni) in the S_0 ground state, featuring the deviation τ_4 from the square planar coordination (for perfect square planar, $\tau_4 = 0$; for perfect tetrahedral $\tau_4 = 1$).

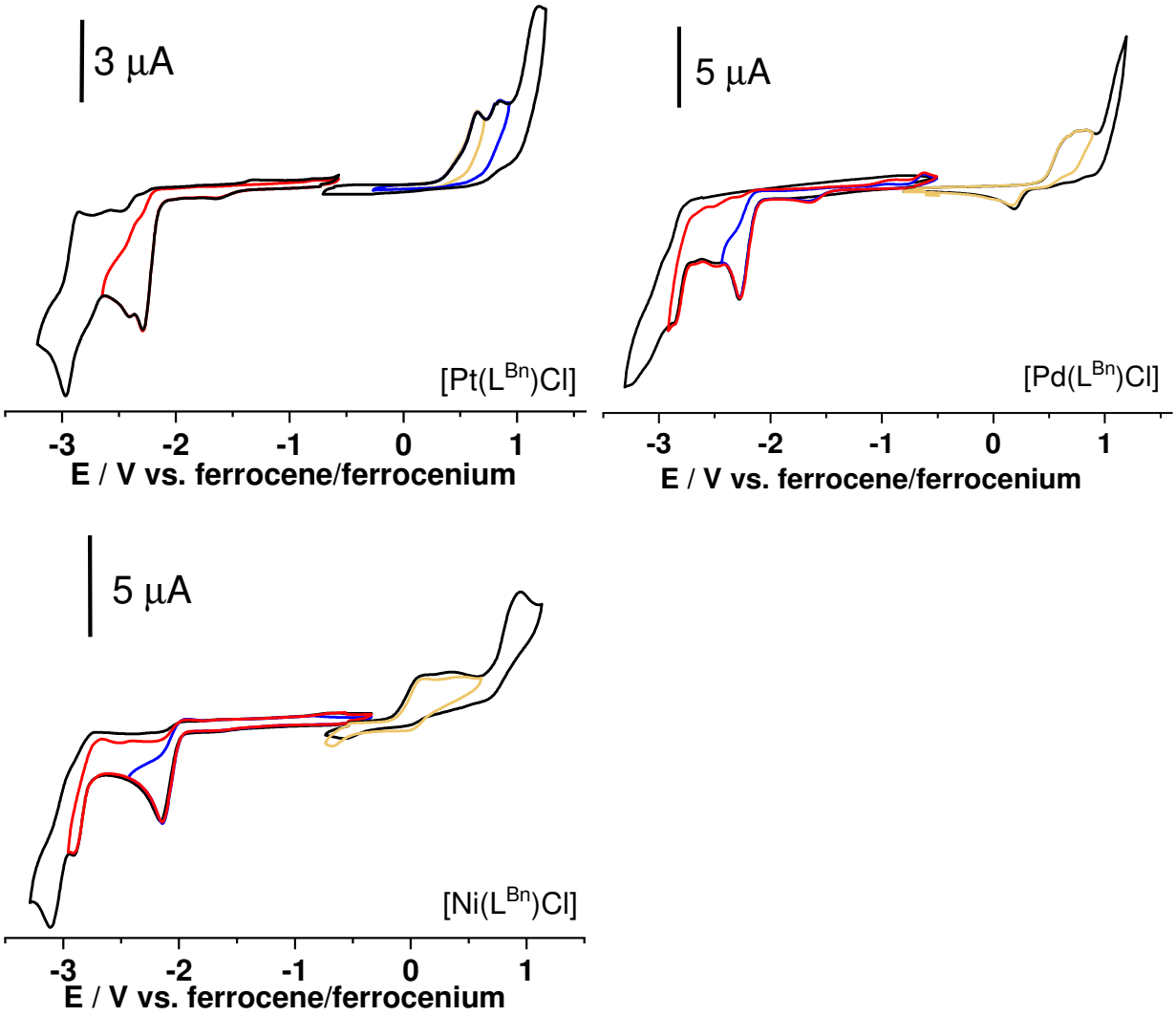

Fig. S20 Cyclic voltammograms of the complexes [M(L^{Bn})Cl] (M = Pt, Pd, and Ni) in *n*-Bu_4NPF_6/THF.

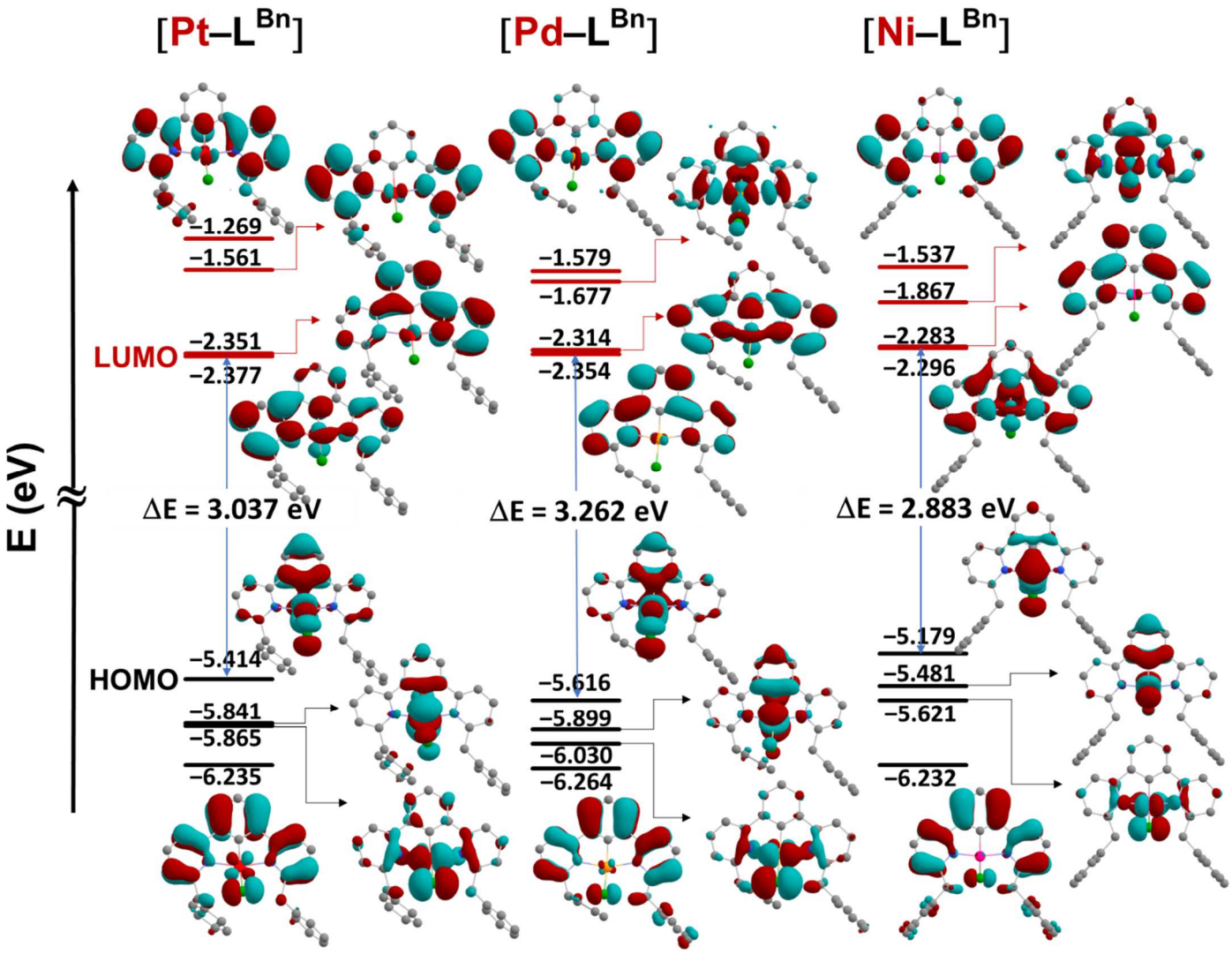

Fig. S21 DFT-calculated energies of the highest occupied (HOMO, black) and lowest unoccupied (LUMO, red) molecular orbitals for [M(L^{Bn})Cl] (M = Pt, Pd, and Ni).

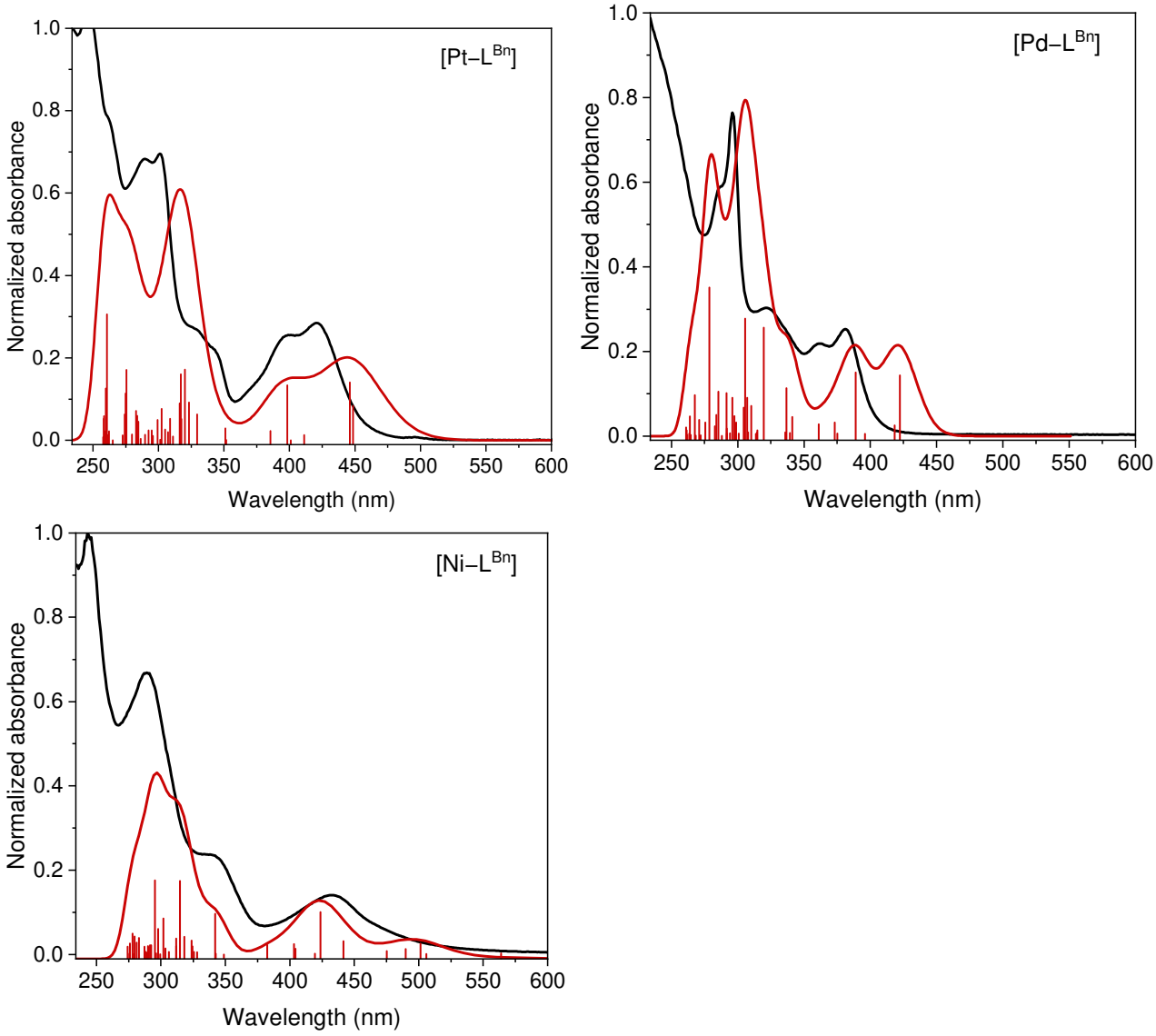

Fig. S22 Experimental UV-vis absorption spectra the complexes [M(L^{Bn})Cl] (M = Pt, Pd, and Ni) measured in THF at 298 K with TD-DFT-calculated transitions on TPSSh/def2-TZVP/CPCM(THF) level of theory (sticks in red).

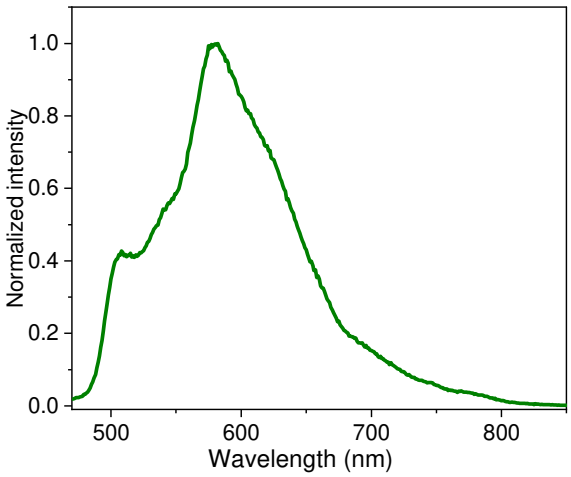

Fig. S23 Emission spectrum of [Pt(L^{Bn})Cl] in CH_2Cl_2 solution at 298 K (λ_{ex} = 376 nm, c = 10^{-5}, 10^{-6}, and 10^{-7} M gave the same results). The spectrum is normalised to the highest intensity.

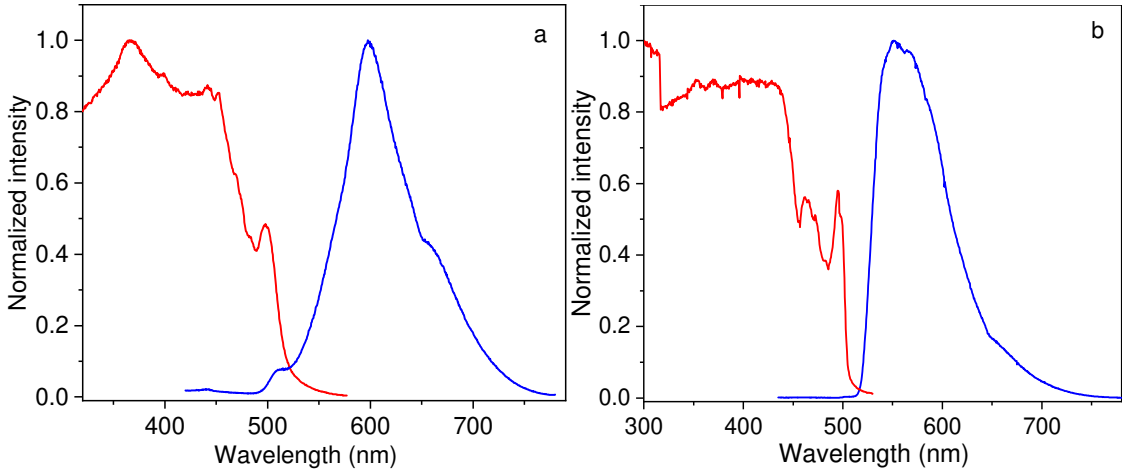

Fig. S24 Photoluminescence emission (blue line) and excitation (red line) spectra of [Pt(L^{Bn})Cl] in solid state at 298 K (a) and at 77 K (b) (λ_{ex} = 400 nm).

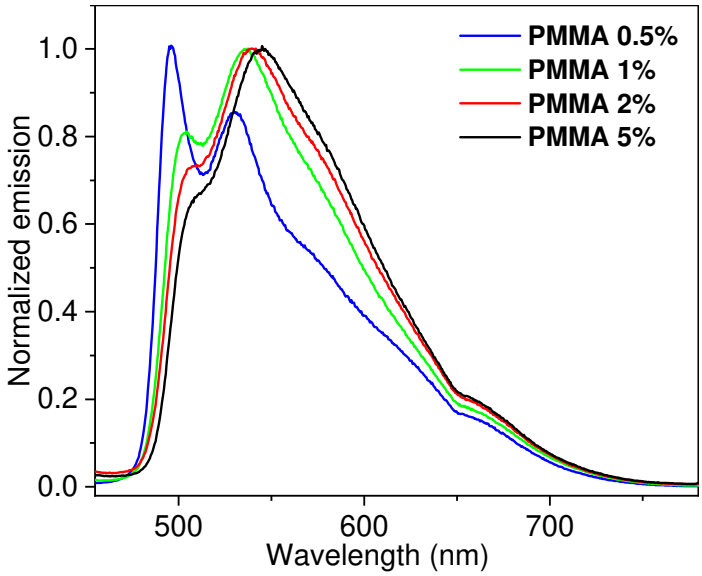

Fig. S25 Photoluminescence spectra of [Pt(L^{Bn})Cl] at different concentrations within PMMA films at 298 K (λ_{ex} = 400 nm).

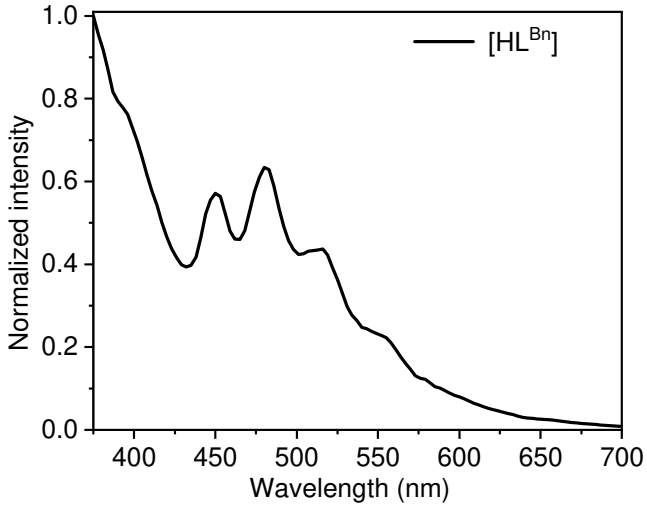

Fig. S26 Photoluminescence emission spectrum of HL^{Bn} in a frozen glassy matrix (2-MeTHF, $c = 10^{-5}$ M, λ_{ex} = 350 nm).

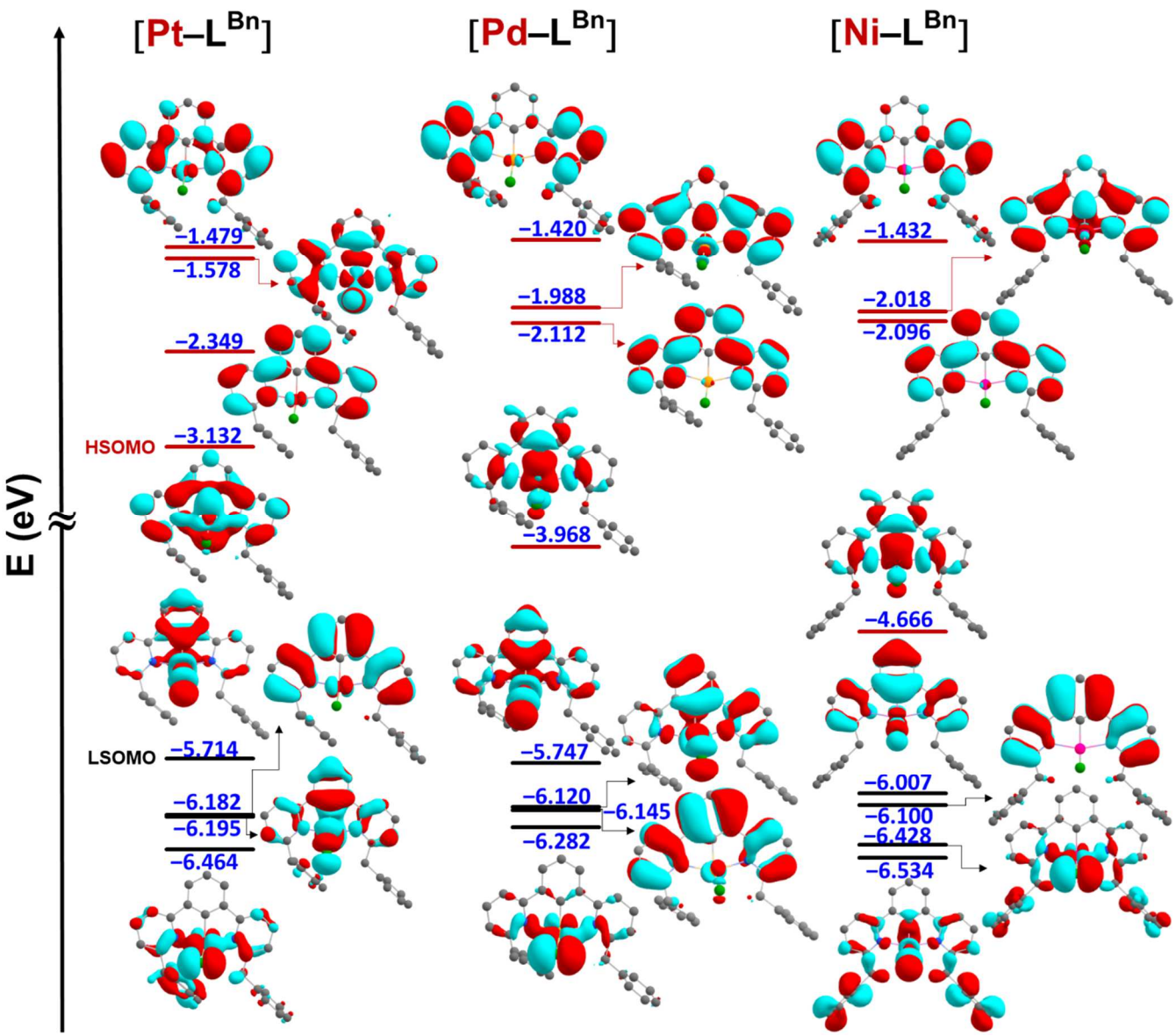

Fig. S27 DFT-calculated energies of the lowest singly occupied (LSOMO, black) and highest singly occupied (LSOMO, red) molecular orbitals for [M(L^{Bn})Cl] (M = Pt, Pd, and Ni).

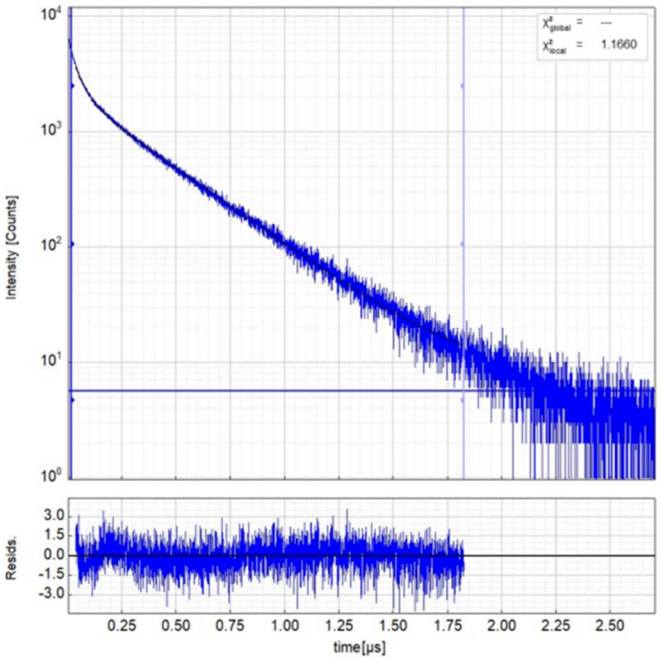

Parameter	Value	Δ	δ
A_1[kCnts/Chnl]	1.9959	±0.0067	0.3%
τ_1[ns]	324.25	±0.82	0.3%
I_1[kCnts]	1 264.0	±3.4	0.3%
A_{Rel1}[%]	55.0	±0.2	0.3%
I_{Rel1}[%]	89.0	±0.2	0.2%
A_2[kCnts/Chnl]	1.6334	±0.0091	0.6%
τ_2[ns]	49.0	±1.1	2.2%
I_2[kCnts]	156.3	±2.6	1.6%
A_{Rel2}[%]	45.1	±0.2	0.3%
I_{Rel2}[%]	11.1	±0.2	1.4%
$Bkgr_{Dec}$[kCnts]	0.0057	±0.0003	4.1%
τ_{AvInt}[ns]	293.97	±0.37	0.1%
τ_{AvAmp}[ns]	200.36	±0.88	0.4%

Fig. S28 Left: Raw (experimental) time-resolved photoluminescence decay of [Pt(L^{Bn})Cl] in fluid CH_2Cl_2 at 298 K (air-equilibrated, λ_{ex} = 376 nm, λ_{em} = 580 nm) including the residuals. Right: Fitting parameters including pre-exponential factors and confidence limits.

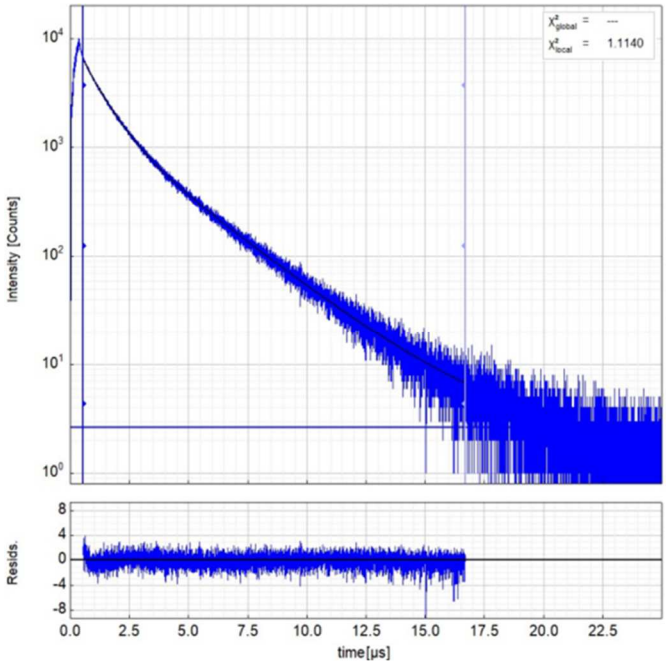

Parameter	Value	Δ	δ
A_1[kCnts/Chnl]	1.830	±0.030	1.6%
τ_1[ns]	2 650	±19	0.7%
I_1[kCnts]	2 425	±23	0.9%
A_{Rel1}[%]	28.9	±0.5	1.4%
I_{Rel1}[%]	56.0	±0.6	1.0%
A_2[kCnts/Chnl]	4.504	±0.024	0.5%
τ_2[ns]	846.5	±7.8	0.9%
I_2[kCnts]	1 907	±25	1.3%
A_{Rel2}[%]	71.2	±0.5	0.6%
I_{Rel2}[%]	44.1	±0.6	1.2%
$Bkgr_{Dec}$[kCnts]	0.0027	±0.0003	10%
τ_{AvInt}[ns]	1 855.8	±4.4	0.2%
τ_{AvAmp}[ns]	1 367.4	±4.1	0.3%

Fig. S29 Left: Raw (experimental) time-resolved photoluminescence decay of [Pt(L^{Bn})Cl] in fluid CH_2Cl_2 at 298 K (Ar-purged, λ_{ex} = 376 nm, λ_{em} = 580 nm) including the residuals. Right: Fitting parameters including pre-exponential factors and confidence limits.

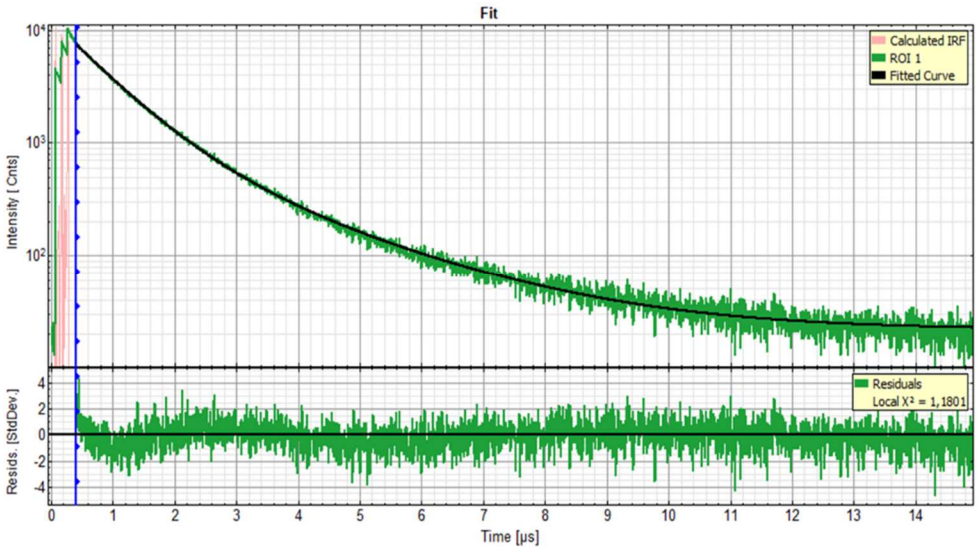

Parameter		ROI 1
t_0[ns]		400,7000 ± ------
A_1 [kCnts]	Limits	1,170 ± 0,018
A_2 [kCnts]	Limits	6,330 ± 0,023
τ_1 [ns]	Limits	2077 ± 16
τ_2 [ns]	Limits	733,0 ± 2,6
$Bkgr_{Dec}$ [Cnts]	Limits	22,0 ± 0,2
I_1 [kCnts]		477,0 ± 3,5
I_2 [kCnts]		907,0 ± 5,1
I_{Sum} [kCnts]		1384,0 ± 1,4
A_{Sum} [kCnts]		7,510 ± 0,024
$\tau_{Av Int}$ [ns]		1196 ± 3
$\tau_{Av Amp}$ [ns]		944,0 ± 1,8
$A_{rel 1}$		0,1565 ± 0,0023
$A_{rel 2}$		0,8435 ± 0,0023

Fig. S30 Raw (experimental) time-resolved photoluminescence decay with the fitting parameters including pre-exponential factors and confidence limits of [Pt(L^{Bn})Cl] as a crystal at 298 K.

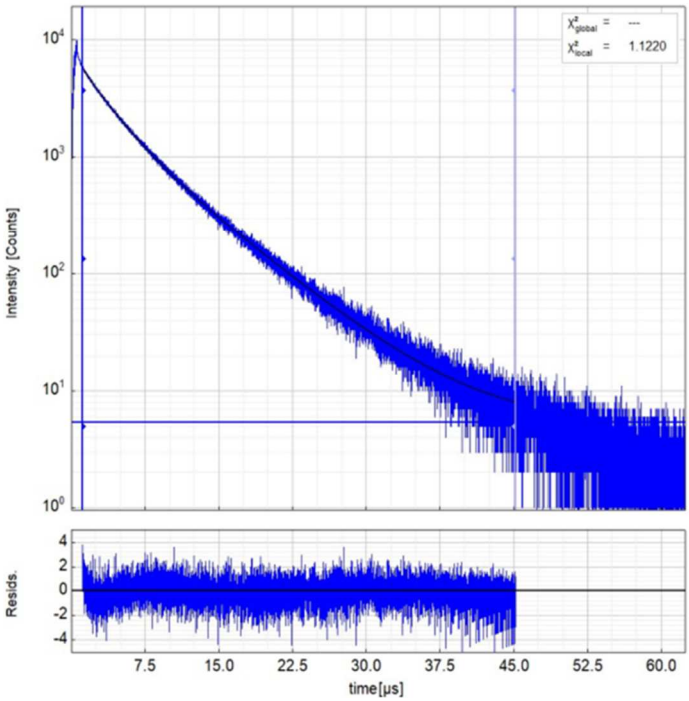

Parameter	Value	Δ	δ
A_1[kCnts/Chnl]	2.382	±0.069	2.9%
τ_1[ns]	6 496	±63	1.0%
I_1[kCnts]	3 869	±75	1.9%
A_{Rel1}[%]	41.8	±1.2	2.7%
I_{Rel1}[%]	63.3	±1.3	1.9%
A_2[kCnts/Chnl]	3.318	±0.060	1.8%
τ_2[ns]	2 706	±46	1.7%
I_2[kCnts]	2 244	±77	3.4%
A_{Rel2}[%]	58.3	±1.2	1.9%
I_{Rel2}[%]	36.8	±1.3	3.4%
$Bkgr_{Dec}$[kCnts]	0.0054	±0.0003	5.0%
τ_{AvInt}[ns]	5 105	±11	0.2%
τ_{AvAmp}[ns]	4 290	±12	0.3%

Fig. S31 Left: Raw (experimental) time-resolved photoluminescence decay of [Pt(L^{Bn})Cl] in a frozen glassy 2-MeTHF matrix (V:V = 1:1) at 77 K, including the residuals (λ_{exc} = 376.7 nm, λ_{em} = 495 nm). Right: Fitting parameters including pre-exponential factors and confidence limits.

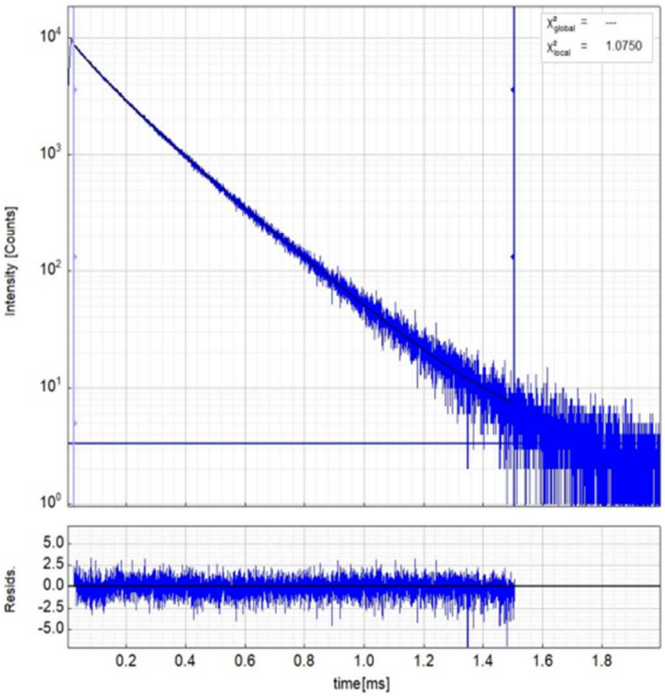

Parameter	Value	Δ	δ
A_1[kCnts/Chnl]	5.58	±0.20	3.6%
τ_1[ns]	204 700	±2 100	1.0%
I_1[kCnts]	4 470	±120	2.6%
A_{Rel1}[%]	64.4	±2.2	3.4%
I_{Rel1}[%]	78.7	±2.1	2.6%
A_2[kCnts/Chnl]	3.09	±0.19	6.0%
τ_2[ns]	100 300	±3 800	3.7%
I_2[kCnts]	1 210	±120	9.6%
A_{Rel2}[%]	35.7	±2.2	6.1%
I_{Rel2}[%]	21.4	±2.1	9.6%
$Bkgr_{Dec}$[kCnts]	0.0034	±0.0004	10%
τ_{AvInt}[ns]	182 410	±270	0.1%
τ_{AvAmp}[ns]	167 460	±410	0.2%

Fig. S32 Left: Raw (experimental) time-resolved photoluminescence decay of [Pd(L^{Bn})Cl] in a frozen glassy 2-MeTHF matrix (V:V = 1:1) at 77 K, including the residuals (λ_{exc} = 376.7 nm, λ_{em} = 700 nm). Right: Fitting parameters including pre-exponential factors and confidence limits.

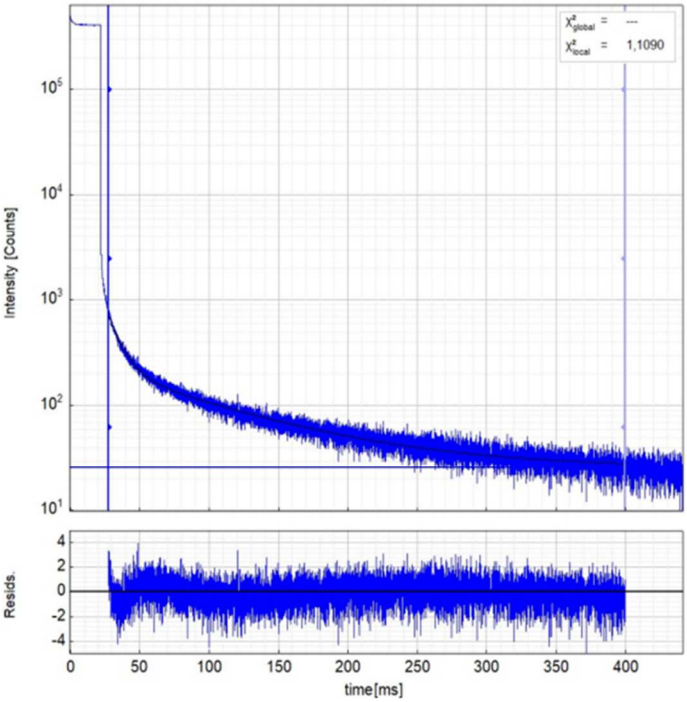

Parameter	Value	Δ	δ
A_1[kCnts/Chnl]	0,1872	±0,0028	1,5%
τ_1[ns]	87 200 000	±1 500 000	1,7%
I_1[kCnts]	497,9	±3,4	0,7%
A_{Rel1}[%]	26,6	±0,4	1,2%
I_{Rel1}[%]	77,3	±0,4	0,4%
A_2[kCnts/Chnl]	0,5168	±0,0072	1,4%
τ_2[ns]	9 320 000	±230 000	2,4%
I_2[kCnts]	147,0	±2,9	1,9%
A_{Rel2}[%]	73,5	±0,4	0,5%
I_{Rel2}[%]	22,8	±0,4	1,5%
$Bkgr_{Dec}$[kCnts]	0,0257	±0,0004	1,4%
τ_{AvInt}[ns]	69 500 000	±1 100 000	1,5%
τ_{AvAmp}[ns]	30 020 000	±450 000	1,5%

Fig. S33 Left: Raw (experimental) time-resolved photoluminescence decay of [Ni(L^{Bn})Cl] in a frozen glassy 2-MeTHF matrix (V:V = 1:1) at 77 K, including the residuals (λ_{exc} = 376.7 nm, λ_{em} = 530 nm). Right: Fitting parameters including pre-exponential factors and confidence limits.

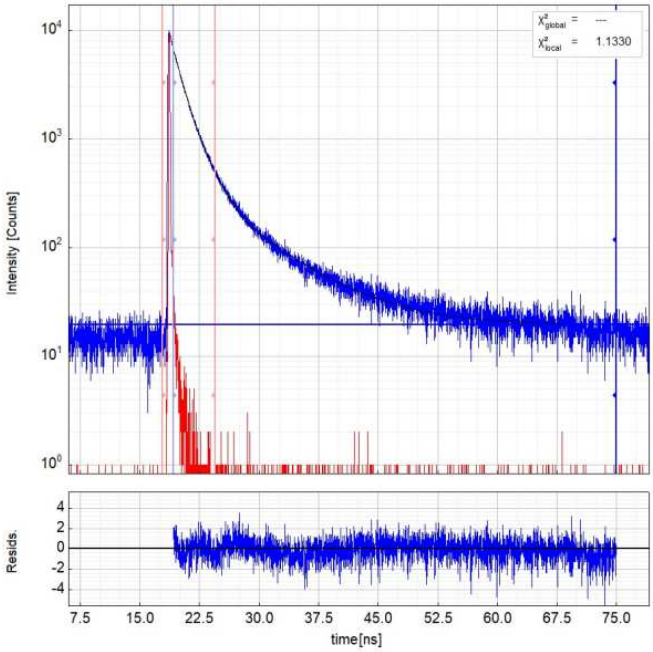

Parameter	Value	Δ	δ
A_1[kCnts/Chnl]	0.488	±0.027	5.5%
τ_1[ns]	7.34	±0.18	2.4%
I_1[kCnts]	223.6	±7.4	3.3%
A_{Rel1}[%]	5.2	±0.4	5.8%
I_{Rel1}[%]	21.6	±0.9	3.8%
A_2[kCnts/Chnl]	8.92	±0.44	4.8%
τ_2[ns]	1.463	±0.014	0.9%
I_2[kCnts]	816	±41	4.9%
A_{Rel2}[%]	94.9	±0.4	0.3%
I_{Rel2}[%]	78.5	±0.9	1.0%
$Bkgr_{Dec}$[kCnts]	0.0194	±0.0004	1.8%
$Bkgr_{IRF}$[Cnts/Chnl]	-11.8	±1.7	14%
$Shift_{IRF}$[ps]	136	±70	51%
A_{Scatt}[kCnts]	-40	±97	235%
τ_{AvInt}[ns]	2.726	±0.039	1.4%
τ_{AvAmp}[ns]	1.767	±0.018	1.0%

Fig. S34 Left: Time-resolved photoluminescence decay (blue) of HL^{Bn} and the instrument response function (IRF, red) in a frozen glassy matrix of 2-MeTHF at 77 K, including the residuals (λ_{ex} = 376 nm, λ_{obs} = 475 nm). Right: Fitting parameters including pre-exponential factors and confidence limits.

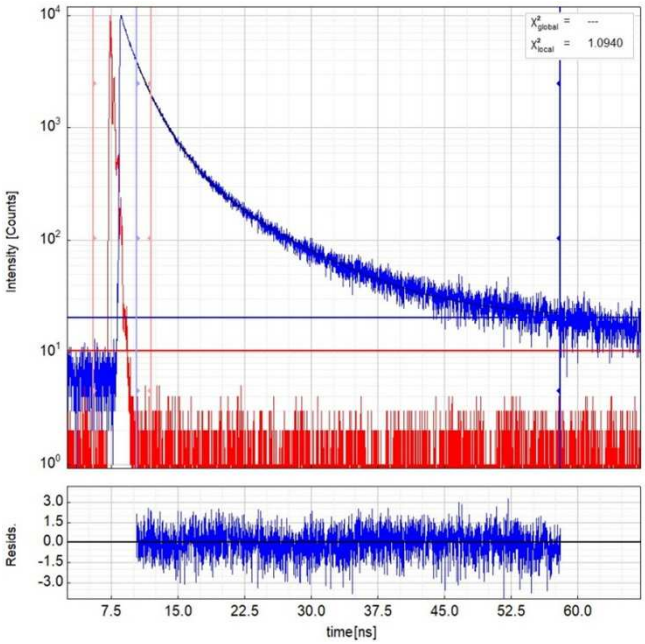

Parameter	Value	Δ	δ
A_1[kCnts/Chnl]	3.434	±0.089	2.6%
τ_1[ns]	8.29	±0.14	1.6%
I_1[kCnts]	1 779	±32	1.8%
A_{Rel1}[%]	8.9	±0.3	2.9%
I_{Rel1}[%]	26.3	±0.5	1.7%
A_2[kCnts/Chnl]	35.48	±0.57	1.6%
τ_2[ns]	2.250	±0.039	1.7%
I_2[kCnts]	4 990	±120	2.4%
A_{Rel2}[%]	91.2	±0.3	0.3%
I_{Rel2}[%]	73.8	±0.5	0.6%
$Bkgr_{Dec}$[kCnts]	0.0205	±0.0009	4.3%
$Bkgr_{IRF}$[Cnts/Chnl]	10.2	±2.7	26%
$Shift_{IRF}$[ps]	-1 129.11	±0.13	0.0%
τ_{AvInt}[ns]	3.838	±0.031	0.8%
τ_{AvAmp}[ns]	2.783	±0.038	1.4%

Fig. S35 Left: Time-resolved photoluminescence decay (blue) of ClL^{Bn} and the instrument response function (IRF, red) in a frozen glassy matrix of 2-MeTHF at 77 K, including the residuals (λ_{ex} = 376 nm, λ_{obs} = 475 nm). Right: Fitting parameters including pre-exponential factors and confidence limits.

Supporting Tables

Table S1 Crystal data and structure refinement for [M(L^{Bn})Cl] (M = Pt or Pd) and Ni(L^{Bn})Cl]·½CH_2Cl_2.[a]

	[Pt(L^{Bn})Cl]	[Pd(L^{Bn})Cl]	[Ni(L^{Bn})Cl]·½CH_2Cl_2
Empirical formula	$C_{30}H_{23}ClN_2Pt$	$C_{30}H_{23}ClN_2Pd$	$C_{30}H_{23}ClN_2Ni{\cdot}0.5(CH_2Cl_2)$
Formula weight	642.04	553.35	548.13
Temperature/K	100(2)	105(2)	100(2)
Crystal system	triclinic	triclinic	monoclinic
Space group	$P\bar{1}$	$P\bar{1}$	$C2/c$
a/Å	8.9466(4)	8.9694(4)	34.298(2)
b/Å	10.2921(5)	10.2495(4)	7.6309(5)
c/Å	14.5835(7)	14.5659(6)	22.2564(14)
α/°	95.206(2)	95.205(2)	90
β/°	107.337(2)	107.440(2)	122.523(2)
γ/°	113.192(2)	112.952(2)	90
Volume/Å^3	1144.63(10)	1143.06(8)	4911.6(6)
Z	2	2	8
ρ_{calc} g/cm^3	1.863	1.608	1.483
μ/mm^{-1}	6.269	0.951	1.0312
F(000)	624.0	560.0	2264.0
Crystal size/mm^3	0.12 × 0.11 × 0.02	0.1 × 0.05 × 0.04	0.32 × 0.13 × 0.04
2Θ range for data collection/°	4.432 to 61.11	4.44 to 61.04	4.34 to 75.6
Index ranges	–12 ≤ h ≤ 12, –14 ≤ k ≤ 14, –20 ≤ l ≤ 20	–11 ≤ h ≤ 11, –12 ≤ k ≤ 12, –18 ≤ l ≤ 18	–58 ≤ h ≤ 58, –13 ≤ k ≤ 13, –38 ≤ l ≤ 38
Reflections collected	41592	17848	158153
Independent reflections	6946 [R_{int} = 0.0500, R_{sigma} = 0.0334]	4626 [R_{int} = 0.0390, R_{sigma} = 0.0337]	13175 [R_{int} = 0.0519, R_{sigma} = 0.0237]
Data/restraints/parameters	6946/0/330	4626/0/235	13174/0/321
Goodness-of-fit on F^2	1.084	1.049	1.083
Final R indexes [I>=2σ (I)]	R_1 = 0.0214, wR_2 = 0.0401	R_1 = 0.0260, wR_2 = 0.0562	R_1 = 0.0386, wR_2 = 0.0972
Final R indexes [all data]	R_1 = 0.0237, wR_2 = 0.0414	R_1 = 0.0293, wR_2 = 0.0579	R_1 = 0.0450, wR_2 = 0.1032
Largest diff. peak/hole / e Å^{-3}	1.16/–2.02	0.49/–0.59	1.77/–1.26
CCDC	2307143	2271328	2258876

[a] From X-ray diffraction on single crystals, measured using MoKα (λ = 0.71073) radiation.

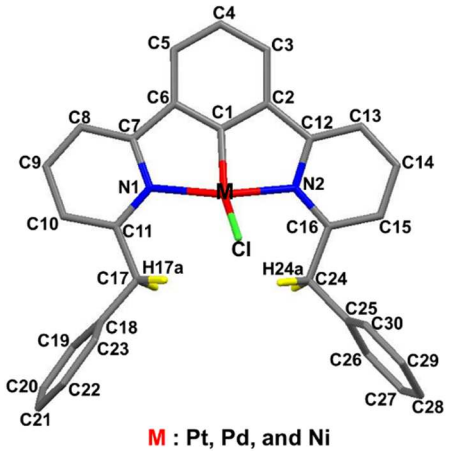

Numbering schemes of the structures of [M(L^{Bn})Cl] (M = Pt, Pd, and Ni) for Table S2.

Table S2 Experimental and DFT-calculated geometries of [M(L^{Bn})Cl] (M = Pt, Pd, Ni).

	[Pt(L^{Bn})Cl]			[Pd(L^{Bn})Cl]			[Ni(L^{Bn})Cl]		
	XRD [a]	DFT [b]		XRD [a]	DFT [b]		XRD [a]	DFT [b]	
bond lengths / Å		S_0	T_1		S_0	T_1		S_0	T_1
M–C1	1.907(2)	1.908	1.947	1.907(2)	1.903	2.044	1.811(1)	1.805	1.916
M–N1	2.072(2)	2.087	2.081	2.105(2)	2.112	2.318	1.945(1)	1.955	2.173
M–N2	2.065(2)	2.088	2.081	2.100(2)	2.114	2.330	1.941(1)	1.955	2.173
M–Cl	2.469(1)	2.505	2.446	2.492(6)	2.522	2.414	2.320(3)	2.325	2.273
Cl···H17a	2.51	2.35	2.60	2.56	2.42	2.92	2.51	2.45	2.72
Cl···H24a	2.67	2.66	2.63	2.72	2.38	2.94	2.61	2.45	2.72
angles / °									
C1–M–Cl	152.1(1)	154.0	121.7	150.3(1)	149.4	114.6	138.5(1)	139.2	121.6
C1–M–N1	80.1(1)	80.3	81.3	79.7(1)	79.8	76.7	82.4(1)	82.5	79.9
C1–M–N2	80.4(1)	80.4	80.9	79.7(1)	79.9	76.5	82.4(1)	82.5	79.9
N1–M–N2	158.6(1)	159.5	161.2	156.7(1)	157.8	152.8	159.7(1)	160.5	156.9
N1–M–Cl	103.5(6)	100.6	97.5	104.6(6)	100.9	97.4	102.6(1)	99.6	100.0
N2–M–Cl	97.9(6)	99.5	97.0	98.7(5)	101.1	97.5	97.7(1)	99.8	100.0
C17–H17a···Cl	142.0(1)	153.9	144.6	143.4(1)	155.5	146.1	149.3(1)	149.3	150.4
C24–H24a···Cl	122.2(1)	112.5	134.5	123.1(2)	162.4	144.6	143.7(1)	149.3	150.4
M–N1–C7–C6	3.2(2)	7.1	5.6	3.4(2)	7.4	5.1	5.4(1)	8.3	7.7
M–N2–C12–C2	–7.8(2)	–5.9	–5.9	–9.1(2)	–6.9	–6.0	–9.4(1)	–8.3	–7.7
M–C1–C6–C7	–12.1(2)	–9.9	12.2	–12.2(2)	–10.7	2.6	–15.1(1)	–13.5	–0.3
M–C1–C2–C12	13.5(3)	9.6	–11.6	13.7(2)	10.9	–2.4	17.4(1)	13.5	0.3
N1–C11–C17–C18	–65.1(3)	–74.1	–68.7	–65.2(3)	–74.5	–71.0	173.2(1)	160.9	163.6
N2–C16–C24–C25	124.2(3)	153.6	167.7	123.7(3)	–160.9	–179.3	–158.6(1)	–160.9	–163.6
C11–C17–C18–C23	144.6(3)	135.9	140.3	143.9(3)	128.5	129.1	–97.4(1)	–76.0	–80.2
C16–C24–C25–C30	146.7(3)	104.0	96.3	147.1(3)	76.5	89.2	72.1(1)	76.0	80.2
τ_4	0.349	0.330	0.547	0.376	0.374	0.657	0.438	0.428	0.578

[a] Experimental data from X-ray diffraction on [M(L^{Bn})Cl] (M = Pt or Pd) and Ni(L^{Bn})Cl] ½CH_2Cl_2 (Table S1). [b] DFT calculations on TPSSh/def2-TZVP/CPCM(THF) level of theory.

Table S3 Redox potentials of the complexes [M(L^{Bn})Cl] (M = Pt, Pd, and Ni).[a]

complex	E_{pc} (Red3)	E_{pc} (Red2)	E_{pc} (Red1)	E_{pa} (Ox1)	E_{pa} (Ox2)	E_{pa} (Ox3)	ΔE (Red1-Red2)	ΔE (Ox1-Red1)
[Pt(L^{Bn})Cl]	–2.97	–2.41	–2.30	0.65	0.85	1.18	0.11	2.95
[Pd(L^{Bn})Cl]	–2.85	–2.50	–2.28	0.73	0.84	1.12	0.22	3.01
[Ni(L^{Bn})Cl]	–3.11	–2.91	–2.15	0.08	0.36	0.94	0.74	2.23

[a] From cyclic voltammetry in n-Bu_4NPF_6/THF. Potentials in V vs. ferrocene/ferrocenium; cathodic peak potentials (E_{pc}) for irreversible reductions; anodic peak potentials (E_{pa}) for irreversible oxidations.

Table S4 Selected UV-Vis absorption maxima of the complexes [M(L^{Bn})Cl] (M = Pt, Pd, and Ni). [a,b]

complex	[Pt(L^{Bn})Cl]	[Pd(L^{Bn})Cl]	[Ni(L^{Bn})Cl]
λ_9 (ε)[b]	246 (57.5)	245 (48.1)	244 (82.9)
λ_8 (ε)[b]	263 (42.8)	–	–
λ_7 (ε)[b]	289 (37.9)	286 (32.6)	289 (55.7)
λ_6 (ε)[b]	301 (38.6)	296 (42.4)	–
λ_5 (ε)[b]	330 (14.8)	321 (16.8)	–
λ_4 (ε)[b]	344 (11.8)	362 (12.2)	343 (19.3)
λ_3 (ε)[b]	399 (14.2)	381 (14.1)	–
λ_2 (ε)[b]	421 (15.8)	–	433 (11.8)
λ_1 (ε)[b]	496 (0.1)	–	–

[a] Measured in THF at 298 K, [b] Absorption maxima λ are given in nm, and molar absorption coefficients ε are given in 10^3 L mol^{-1} cm^{-1}.

Table S5 DFT-calculated energies and compositions of frontier MOs in the S_0 ground state for [M(L^{Bn})Cl] (M = Pt, Pd, and Ni).[a]

complex	MO	energy (eV)	component %			
[Pt(L^{Bn})Cl]			M	NCN = L	Bn = L′	Cl = X
	LUMO+12	1.251	2	48	50	0
	LUMO+11	0.764	7	23	70	0
	LUMO+10	0.392	0	42	58	0
	LUMO+9	–0.302	7	81	12	0
	LUMO+8	–0.599	1	19	80	0
	LUMO+7	–0.657	2	32	66	0
	LUMO+6	–0.736	18	51	29	2
	LUMO+5	–0.763	1	23	75	1
	LUMO+4	–0.827	6	25	69	0
	LUMO+3	–1.269	2	65	33	0
	LUMO+2	–1.561	1	87	12	0
	LUMO+1	–2.351	2	80	18	0
	LUMO	–2.377	3	87	10	0
	HOMO	–5.414	28	39	22	11
	HOMO-1	–5.841	49	37	10	4
	HOMO-2	–5.865	40	26	12	22
	HOMO-3	–6.235	6	65	17	12
	HOMO-4	–6.567	1	25	73	1
	HOMO-5	–6.588	28	20	42	10
	HOMO-6	–6.660	30	21	44	5
	HOMO-7	–6.728	11	14	69	6
	HOMO-8	–6.793	3	7	89	1
	HOMO-9	–6.980	6	22	14	58

	HOMO-10	–7.014	22	45	16	17
	HOMO-11	–7.459	31	33	10	26
	HOMO-12	–7.494	18	55	9	18
[Pd(L^{Bn})Cl]	LUMO+12	1.004	6	55	39	0
	LUMO+11	0.715	6	55	39	0
	LUMO+10	0.364	1	25	74	0
	LUMO+9	–0.327	3	71	26	0
	LUMO+8	–0.616	0	18	82	0
	LUMO+7	–0.647	0	6	94	0
	LUMO+6	–0.743	1	12	87	0
	LUMO+5	–0.775	1	17	82	0
	LUMO+4	–1.247	2	67	31	0
	LUMO+3	–1.579	2	77	21	0
	LUMO+2	–1.677	24	64	10	2
	LUMO+1	–2.314	5	84	11	0
	LUMO	–2.354	1	82	17	0
	HOMO	–5.616	34	40	11	15
	HOMO-1	–5.899	61	31	6	2
	HOMO-2	–6.030	31	22	22	25
	HOMO-3	–6.264	1	75	17	7
	HOMO-4	–6.537	4	14	67	15
	HOMO-5	–6.594	2	23	70	5
	HOMO-6	–6.715	5	17	73	5
	HOMO-7	–6.742	19	12	62	7
	HOMO-8	–6.818	37	19	29	15
	HOMO-9	–6.873	4	24	32	40
	HOMO-10	–6.990	24	36	17	23
	HOMO-11	–7.417	40	37	7	16
	HOMO-12	–7.499	8	76	7	9
[Ni(L^{Bn})Cl]	LUMO+12	1.379	0	68	32	0
	LUMO+11	0.862	8	37	55	0
	LUMO+10	0.443	0	29	71	0
	LUMO+9	–0.307	3	80	17	0
	LUMO+8	–0.643	0	6	94	0
	LUMO+7	–0.656	1	11	88	0
	LUMO+6	–0.743	0	8	92	0
	LUMO+5	–0.779	1	13	86	0
	LUMO+4	–1.158	0	56	44	0
	LUMO+3	–1.537	1	81	18	0
	LUMO+2	–1.867	24	47	25	4
	LUMO+1	–2.283	1	85	14	0
	LUMO	–2.296	6	74	20	0
	HOMO	–5.179	53	20	15	12
	HOMO-1	–5.481	51	44	3	2
	HOMO-2	–5.621	53	15	23	9
	HOMO-3	–6.232	0	77	18	5
	HOMO-4	–6.449	5	30	48	17
	HOMO-5	–6.495	39	13	26	22

	HOMO-6	–6.625	5	12	82	1
	HOMO-7	–6.714	10	29	58	3
	HOMO-8	–6.780	1	5	94	0
	HOMO-9	–6.798	5	22	67	6
	HOMO-10	–7.013	7	16	28	49
	HOMO-11	–7.228	35	15	18	32
	HOMO-12	–7.428	8	69	13	10

[a] LUMO: Lowest Unoccupied Molecular Orbital, and HOMO: Highest Occupied Molecular Orbital. Major contributions (>30%) are marked in grey.

Table S6 DFT-calculated energies and compositions of frontier MOs in the T_1 excited state for [M(L^{Bn})Cl] (M = Pt, Pd, and Ni).[a]

complex	MO	energy (eV)	component %			
[Pt(L^{Bn})Cl]			M	NCN = L	Bn = L′	Cl = X
	HSOMO+3	–1.479	1	88	11	0
	HSOMO+2	–1.578	22	65	9	4
	HSOMO+1	–2.349	2	85	13	0
	HSOMO	–3.132	9	82	9	0
	LSOMO	–5.714	29	44	10	17
	LSOMO-1	–6.182	8	86	6	0
	LSOMO-2	–6.195	35	33	21	11
	LSOMO-3	–6.464	27	25	23	25
[Pd(L^{Bn})Cl]	HSOMO+3	–1.420	1	76	23	0
	HSOMO+2	–1.988	5	79	15	1
	HSOMO+1	–2.112	0	89	11	0
	HSOMO	–3.968	32	64	3	1
	LSOMO	–5.747	36	36	6	22
	LSOMO-1	–6.120	36	45	5	14
	LSOMO-2	–6.145	5	87	6	2
	LSOMO-3	–6.282	33	20	11	36
[Ni(L^{Bn})Cl]	HSOMO+3	–1.432	0	72	28	0
	HSOMO+2	–2.018	3	78	18	1
	HSOMO+1	–2.096	0	81	19	0
	HSOMO	–4.666	18	78	2	2
	LSOMO	–6.007	17	73	4	6
	LSOMO-1	–6.100	0	92	7	1
	LSOMO-2	–6.428	15	17	41	27
	LSOMO-3	–6.534	10	27	49	14

[a] LSOMO: Lowest Singly Occupied Molecular Orbital, and HSOMO: Highest Singly Occupied Molecular Orbital. Major contributions (>30%) are marked in grey.

Table S7 Selected TD-DFT-calculated vertical $S_0 \rightarrow S_n$ transitions for [M(L^{Bn})Cl] (M = Pt, Pd, and Ni).[a]

complex	S_n	oscillator strength f_{osc}	λ (nm)	transitions (major contribution)	Assignment [b]
[Pt(L^{Bn})Cl]	S_1	0.043	448.5	HOMO→LUMO (90%)	π–π* (L), MLCT
	S_2	0.072	446.0	HOMO→L+1 (90%)	π–π* (L), MLCT

	S_3	0.007	411.3	H-1→LUMO (90%)	MLCT, π–π* (L)
	S_5	0.069	398.3	H-2→LUMO (56%)	MLCT
				H-1→L+1 (27%)	MLCT, π–π* (L)
	S_9	0.032	329.6	H-3→L+1 (48%)	π–π* (L)
	S_{10}	0.047	323.3	HOMO→L+3 (63%)	π–π* (L), LL'CT, MLCT, ML'CT
	S_{11}	0.088	320.1	H-5→LUMO (41%)	L'LCT
				H-1→L+2 (30%)	MLCT, π–π* (L)
				H-6→LUMO (16%)	L'LCT, MLCT
	S_{13}	0.082	317.1	H-4→LUMO (52%)	L'LCT
	S_{14}	0.046	316.2	H-5→L+1 (37%)	L'LCT, MLCT
				H-2→L+2 (26%)	MLCT, π–π* (L)
	S_{19}	0.039	302.5	H-6→L+1 (41%)	L'LCT, MLCT
	S_{28}	0.023	284.6	H-10→LUMO (63%)	π–π* (L)
	S_{31}	0.037	282.8	HOMO→L+5 (61%)	LL'CT
	S_{33}	0.088	275.6	H-2→L+6 (44%)	MLCT, ML'CT, π–π* (L), LL'CT
	S_{45}	0.157	260.6	H-3→L+3 (44%)	π–π* (L), LL'CT
[Pd(L^{Bn})Cl]	S_1	0.060	422.2	HOMO→LUMO (93%)	π–π* (L), MLCT
	S_4	0.063	389.0	H-1→LUMO (87%)	MLCT, π–π* (L)
	S_7	0.012	361.0	H-2→LUMO (44%)	MLCT
				HOMO→L+2 (44%)	π–π* (L), MLCT
	S_8	0.019	341.3	H-3→L+1 (65%)	π–π* (L)
	S_{10}	0.047	336.8	H-2→L+2 (65%)	MLCT
	S_{12}	0.107	319.6	H-3→LUMO (61%)	π–π* (L)
	S_{16}	0.030	310.1	H-5→L+1 (50%)	L'LCT
	S_{24}	0.038	296.0	H-3→L+2 (74%)	π–π* (L)
	S_{30}	0.044	285.3	H-10→LUMO (50%)	π–π* (L)
	S_{33}	0.146	278.6	H-2→L+4 (72%)	MLCT, ML'CT
	S_{38}	0.040	267.7	H-5→L+2 (79%)	L'LCT
	S_{40}	0.020	264.0	H-4→L+3 (46%)	L'LCT
				H-11→L+1 (37%)	MLCT, π–π* (L)
[Ni(L^{Bn})Cl]	S_3	0.021	501.4	HOMO→ L+1 (58%)	MLCT
	S_4	0.078	423.7	H-2→LUMO (54%)	MLCT
				H-2→L+2 (26%)	MLCT
	S_{14}	0.074	342.1	H-3→LUMO (90%)	π–π* (L)
	S_{18}	0.026	323.8	H-4→LUMO (82%)	L'LCT, π–π* (L)
	S_{20}	0.134	314.8	H-3→L+1 (52%)	π–π* (L)
				H-1→L+4 (30%)	MLCT, ML'CT, π–π* (L), LL'CT
	S_{29}	0.136	295.3	H-7→L+1 (74%)	L'LCT, π–π* (L)
	S_{37}	0.030	282.9	H-10→LUMO (74%)	XLCT, L'LCT
	S_{43}	0.020	275.9	H-6→L+2 (56%)	L'LCT
				H-11→LUMO (37%)	MLCT, XLCT
	S_{45}	0.014	274.2	HOMO→L+9 (52%)	MLCT

[a] For oscillator strength f > 0.01 except for the lowest-energy transition. M = Pt, Pd, or Ni; L = NCN core; L' = Bn; X = Cl. [b] Sorted from highest to lowest probability.

Table S8 Photophysical properties of [Pt(L^{Bn})Cl] complex at 298 K.

Medium	$\lambda_{em,\,max}$ (nm)	Φ_L	τ (μs)
CH_2Cl_2 (air)	580	n.d.	τ_1 = 0.324 ± 0.001 (55%)

			τ_2 = 0.49 ± 0.001 (45%) τ_{av_amp} = 0.2 ± 0.001
CH_2Cl_2 (Ar-purged)	580	n.d.	τ_1 = 2.650 ± 0.02 (29%) τ_2 = 0.847 ± 0.008 (71%) τ_{av_amp} = 1.367 ± 0.004
Crystalline state	512	n.d.	τ_1 = 2.07 ± 0.02 (16%) τ_2 = 0.733 ± 0.003 (84%) τ_{av_amp} = 0.944 ± 0.002
Solid state	597	-	0.89 (50%), 2.9 (40%), 0.24 (10%)
PMMA 0.5%	496	0.018	0.91 (51%), 3.26 (38%), 0.23 (11%)
PMMA 5%	544	0.012	1.1 (52%), 3.8 (33%), 0.31 (15%)

n.d. = not detected.

Table S9 Calculated coordinates of the optimised singlet ground state structures of the complexes [M(L^{Bn})Cl] (M = Pt, Pd, and Ni).[a]

[Pt(L^{Bn})Cl]				[Pd(L^{Bn})Cl]				[Ni(L^{Bn})Cl]			
atom	coordinates (Å)			atom	coordinates (Å)			atom	coordinates (Å)		
	X	Y	Z		X	Y	Z		X	Y	Z
Pt	0.641753	–0.393854	0.520904	Pd	–0.599232	0.398201	0.461362	Ni	–0.000083	0.933972	0.116271
Cl	–0.245551	0.638134	2.624257	Cl	0.488508	–0.707751	2.449453	Cl	–0.000361	-0.580246	1.880743
N	2.523934	0.501729	0.416204	N	–2.578636	–0.315682	0.641999	N	–1.926947	1.155627	–0.130294
C	2.87833	1.770324	0.736663	N	1.007765	1.542548	–0.298837	N	1.926761	1.155806	–0.130164
N	–0.947993	–1.668476	0.061979	C	–1.555125	1.870147	–0.274658	C	–0.00016	2.719339	–0.152528
C	0.899527	–2.906447	–0.80153	C	–0.83005	2.994361	–0.678073	C	1.219681	3.390378	–0.076093
C	4.214137	2.16486	0.709651	C	–1.52977	4.163467	–0.998828	C	1.218344	4.78674	0.010712
H	4.459844	3.17788	1.000619	H	–1.004419	5.054957	–1.323104	H	2.145577	5.347293	0.064736
C	1.577302	–1.727085	–0.473187	C	–2.919536	4.190085	–0.890211	C	–0.000292	5.468417	0.041815
C	1.812224	2.781661	1.05277	H	–3.455568	5.097472	–1.14086	H	–0.000344	6.549919	0.108049
H	1.098711	2.358022	1.759789	C	–3.6296	3.076031	–0.444911	C	–1.218862	4.786623	0.010727
H	2.296709	3.637224	1.532174	H	–4.70777	3.13674	–0.346436	H	–2.146148	5.347089	0.064749
C	–1.039032	3.860827	1.238275	C	–2.943721	1.899788	–0.120312	C	–1.220066	3.390259	–0.076072
H	–2.119187	3.943779	–1.18756	C	–3.511028	0.655281	0.38347	C	–2.342736	2.46273	–0.096084
C	3.485526	–0.352628	–0.080936	C	–4.870371	0.42127	0.568666	C	–3.690744	2.796742	–0.124879
C	1.059867	3.26092	–0.180425	H	–5.581068	1.213547	0.375139	H	–3.98792	3.835925	–0.07188
C	2.969002	–1.621369	–0.5753	C	–5.293083	–0.827878	0.991167	C	–4.631893	1.785024	–0.241789
C	4.826535	0.017372	–0.120246	H	–6.345483	–1.0283	1.152444	H	–5.68974	2.018171	–0.265746
H	5.558554	-0.686813	–0.492407	C	–4.347696	–1.826699	1.174414	C	–4.199448	0.471914	–0.363789
C	–2.277069	–1.447799	0.210047	H	–4.642919	–2.826407	1.465912	H	–4.905199	–0.336286	–0.500488
C	5.202741	1.278502	0.305783	C	–2.993905	–1.556511	0.975949	C	–2.837808	0.176849	–0.318724
H	6.243654	1.578174	0.295316	C	0.613085	2.791001	–0.707751	C	2.342435	2.462952	–0.096121
C	1.629619	–3.976143	–1.329283	C	1.537157	3.736196	–1.139265	C	3.690409	2.797084	–0.125108
H	1.142566	–4.904593	–1.606285	H	1.198934	4.720287	–1.435025	H	3.987494	3.836302	–0.072276
C	–4.13543	0.286388	0.242289	C	2.878634	3.395157	–1.196383	C	4.631638	1.785441	–0.242023
C	1.728686	3.6365	–1.348976	H	3.616435	4.117106	–1.525536	H	5.68946	2.018685	–0.266145
H	2.809293	3.552914	–1.402909	C	3.258407	2.105291	–0.857642	C	4.199303	0.472274	–0.363801
C	–3.201261	–2.445785	–0.088638	H	4.290734	1.790907	–0.930164	H	4.905113	–0.335879	–0.50047
H	–4.252702	–2.236708	0.054111	C	2.304382	1.185601	–0.424147	C	2.837696	0.177091	–0.318531
C	–0.363249	4.232924	–2.397086	C	–1.983031	–2.666848	1.070159	C	–2.318874	–1.220721	–0.566763
H	–0.911989	4.60805	–3.253574	H	–1.121923	–2.32464	1.647031	H	–1.435182	–1.363098	0.060677

C	–0.331629	3.37609	–0.140311	H	–2.444796	–3.499435	1.607972	H	–1.979175	–1.254638	–1.60846
H	–0.859804	3.07975	0.759255	C	–1.508159	–3.147893	–0.293328	C	–3.311553	–2.331999	–0.325623
C	–1.428563	–3.865551	–0.812721	C	–2.412562	–3.540716	–1.28457	C	–3.919249	–2.997502	–1.392211
H	–1.06333	–4.787924	–1.244089	H	–3.479592	–3.481956	–1.095364	H	–3.676313	–2.707337	–2.409605
C	3.011202	–3.856216	–1.489501	C	–1.960829	–4.007538	–2.515199	C	–4.828176	–4.029395	–1.166319
H	3.571662	–4.686794	–1.901283	H	–2.676752	–4.308495	–3.272131	H	–5.288568	–4.535682	–2.007493
C	–5.65588	1.082572	–1.471919	C	–0.594111	–4.089758	–2.775035	C	–5.141211	–4.410335	0.135114
H	–5.823178	1.419674	–2.488903	H	–0.242055	–4.453092	–3.733942	H	–5.846391	–5.214149	0.3139
C	–4.376037	0.717875	–1.066289	C	0.314375	–3.701782	–1.794738	C	–4.53809	–3.75535	1.207563
H	–3.552258	0.774018	–1.770814	H	1.380235	–3.762059	–1.985999	H	–4.771152	–4.050665	2.224594
C	1.024263	4.117778	–2.44877	C	–0.141064	–3.232543	–0.564071	C	–3.631134	–2.725659	0.978168
H	1.560257	4.404613	–3.346834	H	0.56762	–2.927387	0.197876	H	–3.159777	–2.224573	1.817272
C	3.688475	–2.698902	–1.102677	C	2.66723	–0.257201	–0.165409	C	2.318847	–1.220593	–0.566091
H	4.767006	–2.655799	–1.207105	H	2.36644	–0.823293	–1.05462	H	1.435415	–1.362932	0.061741
C	–2.778237	–3.673525	–0.575279	H	2.04944	–0.618021	0.661411	H	1.978682	–1.254741	–1.607627
H	–3.494837	–4.455388	–0.795994	C	4.125912	–0.514156	0.124988	C	3.311836	–2.331666	–0.325245
C	–0.527246	–2.850077	–0.512956	C	4.964237	–1.078457	–0.838841	C	3.919486	–2.996877	–1.392047
C	–2.739894	–0.089484	0.684318	H	4.560455	–1.330794	–1.814342	H	3.676243	–2.706673	–2.409357
H	–2.025063	0.653377	0.32478	C	6.30792	–1.323976	–0.562627	C	4.828759	–4.028534	–1.166484
H	–2.671764	–0.059515	1.77363	H	6.942647	–1.764549	–1.323487	H	5.289101	–4.534591	–2.007824
C	–6.491371	0.596966	0.732876	C	6.832221	–1.007024	0.686989	C	5.142202	–4.409539	0.134834
H	–7.310886	0.552174	1.441517	H	7.876739	–1.198531	0.905319	H	5.847652	–5.213172	0.313365
C	–5.207652	0.233593	1.135469	C	6.004164	–0.447049	1.658332	C	4.539139	–3.754848	1.207491
H	–5.034989	–0.090394	2.156822	H	6.402692	–0.204066	2.637122	H	4.772516	–4.050207	2.224437
C	–6.719216	1.021724	–0.572754	C	4.663142	–0.204017	1.378948	C	3.631835	–2.725385	0.978424
H	–7.716232	1.308664	–0.887285	H	4.022739	0.224702	2.142801	H	3.16053	–2.224544	1.817701

[a] DFT calculations on TPSSh/def2-TZVP/CPCM(THF) level of theory.

Table S10 Calculated coordinates of the optimised triplet excited state structures of the complexes [M(L^{Bn})Cl] (M = Pt, Pd, and Ni).[a]

[Pt(L^{Bn})Cl]				[Pd(L^{Bn})Cl]				[Ni(L^{Bn})Cl]			
atom	coordinates (Å)			atom	coordinates (Å)			atom	coordinates (Å)		
	X	Y	Z		X	Y	Z		X	Y	Z
Pt	0.619226	–0.290175	0.3077	Pd	–0.538465	0.182863	0.292773	Ni	–0.000002	0.675309	–0.043261
Cl	–0.036826	0.175082	2.618083	Cl	–0.033697	–0.014027	2.644958	Cl	–0.000017	–0.585202	1.848201
N	2.507565	0.580724	0.380826	N	–2.819653	–0.196751	0.445992	N	–2.129201	1.063273	–0.240154
C	2.844533	1.835855	0.79275	N	1.313881	1.459998	–0.311208	N	2.129198	1.063278	–0.240131
N	–0.922459	–1.617154	–0.132008	C	–1.351603	1.975822	–0.255845	C	–0.000005	2.590087	0.026221
C	0.981794	–2.958003	–0.662546	C	–0.504386	3.001425	–0.671296	C	1.214448	3.266461	0.003128
C	4.172109	2.208968	0.923759	C	–1.073044	4.206136	–1.10967	C	1.218658	4.668041	0.014949
H	4.396677	3.216439	1.250718	H	–0.457599	5.031774	–1.450993	H	2.141544	5.238871	–0.004082
C	1.682518	–1.852834	–0.159068	C	–2.45994	4.348814	–1.123182	C	–0.000008	5.349937	0.032322
C	1.744492	2.826159	1.065794	H	–2.895273	5.280267	–1.466254	H	–0.00001	6.434043	0.038482
H	1.035926	2.393149	1.775751	C	–3.297629	3.312365	–0.713905	C	–1.218673	4.668038	0.014936
H	2.196728	3.696606	1.550459	H	–4.371707	3.45954	–0.754139	H	–2.14156	5.238866	–0.004106
C	–1.102308	3.931348	–1.219655	C	–2.739381	2.103461	–0.273078	C	–1.214459	3.266458	0.003115
H	–2.177418	4.059043	–1.156935	C	–3.524445	0.929043	0.171045	C	–2.400938	2.387675	–0.081704
C	3.52021	–0.321425	0.065707	C	–4.913499	0.945561	0.318392	C	–3.717407	2.841715	–0.01868
C	0.987894	3.283133	–0.171326	H	–5.472139	1.847048	0.10525	H	–3.920828	3.895494	0.119921

C	3.051354	–1.6277	–0.367284	C	–5.567736	–0.196804	0.751893	C	–4.755973	1.928928	–0.127352
C	4.857342	0.043906	0.175203	H	–6.644304	–0.195388	0.876859	H	–5.785605	2.264086	–0.078005
H	5.620241	–0.682343	–0.075284	C	–4.828474	–1.339675	1.030733	C	–4.465424	0.582092	–0.300658
C	–2.261114	–1.40371	–0.004138	H	–5.308226	–2.246678	1.376761	H	–5.253882	–0.152891	–0.393282
C	5.199404	1.311084	0.616135	C	–3.445113	–1.307194	0.864094	C	–3.132598	0.178155	–0.355108
H	6.237546	1.60095	0.719716	C	0.950267	2.726328	–0.631326	C	2.40093	2.387681	–0.08168
C	1.730513	–3.960158	–1.285639	C	1.922067	3.692208	–0.901538	C	3.717398	2.841725	–0.018643
H	1.255277	–4.85082	–1.68247	H	1.630372	4.704369	–1.147896	H	3.920814	3.895504	0.119959
C	–4.157454	0.292001	0.207554	C	3.261896	3.342896	–0.842712	C	4.755967	1.928941	–0.127306
C	1.652978	3.59242	–1.360837	H	4.027664	4.082487	–1.046303	H	5.785597	2.264101	–0.077951
H	2.728641	3.462835	–1.423287	C	3.616191	2.038605	–0.519306	C	4.465422	0.582103	–0.300615
C	–3.165932	–2.430155	–0.219035	H	4.653753	1.736536	–0.469044	H	5.253884	–0.152877	–0.393233
H	–4.222689	–2.222781	–0.116932	C	2.609024	1.113215	–0.257216	C	3.132598	0.178163	–0.355077
C	–0.429826	4.235278	–2.400239	C	–2.58789	–2.515924	1.151447	C	–2.724369	–1.263852	–0.58152
H	–0.976364	4.602612	–3.261449	H	–1.770128	–2.205089	1.807784	H	–1.861422	–1.45672	0.063516
C	–0.397226	3.456691	–0.116121	H	–3.19198	–3.246967	1.696629	H	–2.371336	–1.348672	–1.615375
H	–0.926061	3.219997	0.801299	C	–2.004742	–3.167073	–0.090588	C	–3.800517	–2.291085	–0.328543
C	–1.356373	–3.909711	–0.745475	C	–2.819595	–3.533046	–1.166476	C	–4.523082	–2.852523	–1.383647
H	–0.972278	–4.877106	–1.043089	H	–3.884656	–3.327796	–1.128681	H	–4.303494	–2.548184	–2.402221
C	3.114112	–3.800864	–1.426391	C	–2.280715	–4.156485	–2.28744	C	–5.51672	–3.799688	–1.145058
H	3.684645	–4.580175	–1.917807	H	–2.928159	–4.433565	–3.112079	H	–6.065316	–4.226537	–1.977333
C	–6.054942	0.930021	–1.1629	C	–0.914478	–4.425017	–2.352322	C	–5.800803	–4.199922	0.157515
H	–6.455021	1.215644	–2.129458	H	–0.494781	–4.910006	–3.226349	H	–6.571527	–4.938799	0.345609
C	–4.696856	0.655424	–1.029923	C	–0.094007	–4.065393	–1.287577	C	–5.083818	–3.649361	1.218104
H	–4.045759	0.728497	–1.895329	H	0.970392	–4.269263	–1.326882	H	–5.293665	–3.960675	2.235399
C	0.951113	4.062993	–2.466906	C	–0.63724	–3.441023	–0.165991	C	–4.09235	–2.703706	0.975565
H	1.484111	4.29788	–3.381687	H	0.006434	–3.164008	0.662579	H	–3.533487	–2.284086	1.805861
C	3.774803	–2.644598	–0.999463	C	2.885188	–0.335024	0.099187	C	2.724371	–1.263844	–0.58149
H	4.838764	–2.543158	–1.184906	H	2.372	–0.955332	–0.643467	H	1.861437	–1.456718	0.063562
C	–2.71766	–3.701144	–0.586458	H	2.387442	–0.528762	1.05528	H	2.371316	–1.348659	–1.615338
H	–3.42256	–4.506666	–0.750932	C	4.33953	–0.725967	0.177262	C	3.800527	–2.291076	–0.328541
C	–0.463864	–2.870456	–0.515844	C	5.010076	–1.2155	–0.946891	C	4.523092	–2.852484	–1.383662
C	–2.684044	0.000632	0.350835	H	4.472789	–1.323013	–1.883977	H	4.303497	–2.548123	–2.402228
H	–2.103647	0.680663	–0.285579	C	6.354661	–1.57072	–0.877776	C	5.516739	–3.799647	–1.145098
H	–2.359754	0.203162	1.375834	H	6.857404	–1.952183	–1.759582	H	6.065335	–4.226472	–1.977386
C	–6.371004	0.485672	1.181904	C	7.050328	–1.441527	0.321803	C	5.800831	–4.199908	0.157464
H	–7.017792	0.421758	2.049871	H	8.096459	–1.720324	0.378389	H	6.571561	–4.938783	0.345538
C	–5.010813	0.214229	1.310906	C	6.391751	–0.958515	1.450062	C	5.083846	–3.649377	1.218069
H	–4.605286	–0.057931	2.280144	H	6.92358	–0.861289	2.390004	H	5.293699	–3.960713	2.235356
C	–6.897178	0.843955	–0.056373	C	5.047089	–0.604939	1.376532	C	4.092369	–2.703724	0.975555
H	–7.954708	1.059962	–0.157939	H	4.538394	–0.234653	2.260897	H	3.533506	–2.284128	1.805864

[a] DFT calculations on TPSSh/def2-TZVP/CPCM(THF) level of theory.